

Response to the second round review of

Upwelling characteristics in the Gulf of Finland (Baltic Sea) as revealed by Ferrybox measurements in 2007–2013

General:

The paper is now much better to read and less cluttered. However, I feel that it still needs more work, especially the discussion section. The authors should be commended for including more physics in this version of the paper as compared to the previous version. The authors have several hypotheses to explain the different wind strengths needed for the N and S shore upwelling and to explain the spatial variability in the structure of the upwelling. I feel that the authors can improve on this, as their arguments are not yet clear. It would be helpful to the reader to include some conceptual diagrams that explain their hypotheses. Are there any references that have looked at this in other straits elsewhere on this planet?

Response: Thank you. Your comments have forced us to be more precise in formulating what are the main results of the study. We tried to include more physics in the discussion of the results. We give our explanations below answering the detailed questions and comments.

Detailed comments

Figure 1. If the colorbar at (b) does not apply to the colorbar at (a), please add colorbar to (a).

Response: Color bar for (a) is added in the revised manuscript.

L102. Please mention how this paper addresses the unknowns in the literature regarding the upwelling. As it is stated now, the goal is to just present observations, but not really to explain them.

Response: We are sorry if the main aim was not clearly formulated in the manuscript. The study has two main aims:

1) To show that the Ferrybox technology can be successfully used to describe a major dynamical feature in the stratified estuaries (in our case, the Gulf of Finland). We think that such analysis has not been published until now, and it is not obvious due to many details that you have to consider. Furthermore, only using such routine measurements one would be able to reveal statistical characteristics of upwelling events, such as their duration, extent, intensity, etc. Data from point measurements do not allow such analysis and remote sensing (although the best in assessing the extent of a single event) data have considerable gaps in our area due to the cloud cover.

2) To show that the upwelling characteristics differ along the two coasts in the sense of the reaction to the wind forcing and give an explanation for this finding. Several studies based on modeling and just applying wind data have suggested that the upwelling events along the northern coast of the Gulf of Finland are more frequent than along the southern coast. We show (based on the in situ data covering the both coastal areas) that the frequencies and intensities of the coastal upwelling events are similar along the both coasts although the wind forcing suggests more events (and more intense events) along the northern coast. Some differences of the upwelling dynamics along the two coasts have been noted earlier and they have been explained by the differences in stratification and bottom slope (we cited some of the recent results and the theoretical background in the manuscript, both, in the introduction and the discussion chapter).

We suggest that the general thermohaline structure (a deeper position of the thermocline in the northern gulf) would be the reason why the initiation of the upwelling along the northern coast needs (on average) a stronger wind impulse. We also suggest that for a stronger wind impulse (during a longer period), the estuarine character of the basin has a significant influence on the outcome. If strong southwesterly winds prevail, a general downward movement of the thermocline in the gulf occurs since the southwesterly winds cause inflow in the surface layer and outflow in the sub-surface layers (see e.g. Elken et al., 2003; Lips et al., 2008; Liblik et al., 2013, etc.). In contrary, the down-estuary winds cause a general upward movement of the thermocline in the gulf. Consequently, the up-estuary southwesterly winds, on the one hand cause upwelling along the northern coast, but on the other hand downwelling in the whole gulf (which could weaken the outcome). In the case of down-estuary easterly-northeasterly winds, a general upwelling in the whole gulf supports the coastal upwelling along the southern coast.

L215. Is UI computed using the deviation from the mean of the daily transects or the mean of one single transect? In Figure 2, L312 you use “daily transect mean”. It is somewhat confusing.

Response: It is pointed out that UI is computed for each crossing (L216-217): “For each crossing, the average water temperature and horizontal profile of temperature deviations from the average were found”. Just a few lines later (L220-221), it is explained once again that “... the temperature deviation ... from the average temperature of the crossing” is used in the formula.

Two values obtained within a day (if data from two crossings were available) were averaged to include all days in the analysis with the same weight when describing the seasonal mean distribution and variability. The problem was that occasionally data from only one crossing a day were available. Thus, usually the daily average means an average of two crossings or just one crossing if the second was missing. Where relevant we tried to point it out (and repeat it) in the text and figure captions to avoid misunderstanding.

L243. Remind the reader again that PT100 is a temperature sensor.

Response: OK, done in the remaining sentence.

L243-246. It is unclear what you say here regarding, precision, uncertainty, '25 times'. Please omit or be clearer.

Response: Detailed characteristics of PT100 are given earlier (see L131-134). To avoid misunderstanding and confusion we deleted the sentence where the precision was mentioned. The purpose of mentioning of the uncertainty of the upwelling index estimates is to show that the uncertainty in estimates (due to the accuracy of the sensor) is much lower than the obtained values and even 25 times less the used threshold. The term “uncertainty“ refers here to the uncertainty of the UI estimates. If the accuracy is 0.04 °C then (when summing 40 values), the uncertainty of the estimate is $40 \times 0.04 = 1.6$ °C. This value is 25 times less than the threshold value (40 °C) used in the paper to define whether an upwelling event is occurring or not.

L248-258. This relates to my previous comments in the first round (see comment P10, L24). The authors can compute $w = 1/f * (d\tau_y/dx - d\tau_x/dy)$ and see how w compares to the w estimated from upwelling. The authors did not even come up with quantitative back of the envelope calculations and used qualitative arguments to reject this idea. I do not think it is hard to show quantitatively that wind shear does not play a role. Maybe the wind shear affects the frontal dynamics related to the discussion of Figure 8?

I still have some un-addressed questions regarding the wind. Why not use an area averaged wind speed locally at the ferry transect? Why not use the weather station instead of the model data if a model data point is chosen close to the weather station (L252)?

Response: We do not think it is necessary to calculate the vertical velocity due to the Ekman pumping in the context of the present study. It is known (see e.g. in Leppäranta and Myrberg, 2008. Physical Oceanography of the Baltic Sea. Springer, p. 276-277) that in the Baltic Sea, the coastal upwelling could create vertical motions with an order of magnitude of 10^{-5} to 10^{-4} m s⁻¹ while the Ekman pumping could contribute at about 10^{-6} m s⁻¹. Thus, the latter is about 1-2 orders of magnitude lower.

As regard to the second comment, we wanted to keep the present analysis of the influence of the wind on coastal upwelling comparable with some previous studies (Uiboupin and Laanemets, 2009; Lips et al., 2008) and used data from Kalbadagrund. We preferred to use the modeled wind data since it was available at 10 m level. To show that the HIRLAM outcome at Kalbadagrund and the ferrybox transect are almost identical, we present here the graphs of wind stress from those two model points (see below). We do not think we have to recalculate the CSW values since it will not change the results.

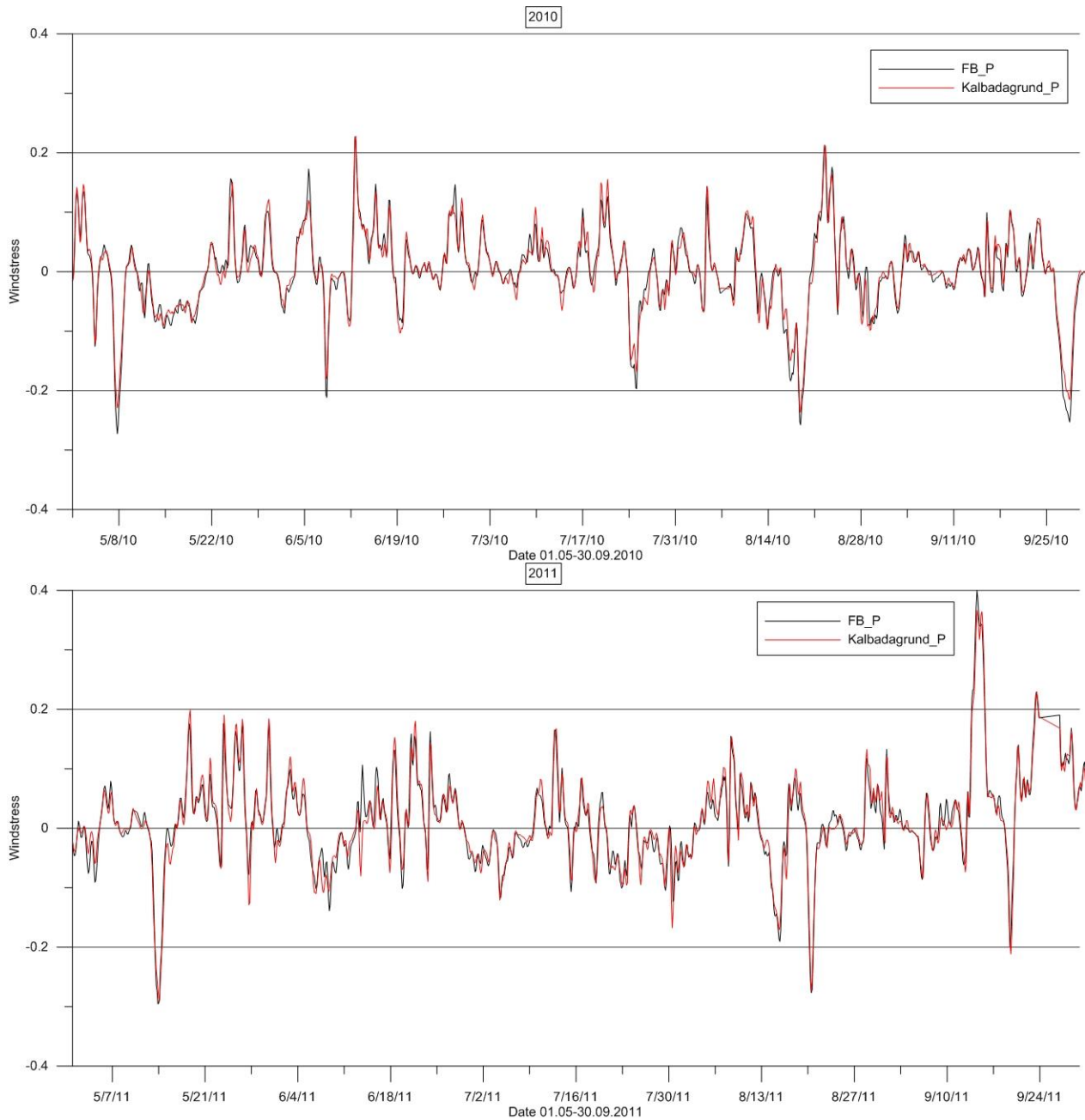


Fig. A. Along-gulf wind stress time series in 2010 and 2011 based on the HIRLAM data from the two model points (at Kalbadagrund and the Ferrybox transect).

L256-258. The English is not clear in this sentence.

Response: The sentence is adjusted to match better the results of an analysis by Keevallik and Soomere (2010).

L210. "longest" please specify how many days.

Response: We guess this comment refers to L280. We changed the text and replaced the two sentences by the following sentence "Within the analyzed years 2007-2013, the surface layer temperature was the highest in summer 2010 (Fig. 2) when the period with the average along-transect temperature > 20 °C was 35 days".

L307. Use of 'course' here and elsewhere sounds out of place. Maybe use 'trends'?

Response: OK, "seasonal course" is replaced by "seasonal trend".

L312. This is Figure 3.

Response: Yes, it is corrected now.

L317. Is this the daily mean or transect-mean T?

Response: This sentence refers to the seasonal averages of temperature and salinity deviations in a cell.

L318. Please indicate how RMSE is computed (show a formula).

Response: We hope that it is not necessary to include a formula for the RMSE calculation in the paper. We explain the calculation procedure here in more detail. Measurements from one crossing are pre-processed to get a series (horizontal profile) consisting of 140 temperature values (one temperature value in each of the 0.5 km cells). Then, the arithmetic mean of the temperature of the crossing is subtracted from each temperature value to get a series (horizontal profile) of temperature deviations. After that, a seasonal average ($dT_{average}$) of these temperature deviations for each cell is estimated, and the corresponding RMSE of this estimate is given as $RMSE = 1/N * \sum_{i=1:N} (dT_i - dT_{average})^2$, where $i=1:N$ is the number of the crossing. Thus, the average ($dT_{average}$) and RSME are estimated using up to $N=300$ values of dT in a cell.

L389. The two subsequent dashes may be confusing?

Response: Changed to brackets. We hope it is less confusing.

L408. Use of 'column' is confusing. Use something like "top and bottom of each subplot"

Response: Thank you. Changed as suggested.

L420. 'was revealed'. English. It sounds like it was revealed in the past and not in this paper.

Response: Changed to "Seasonal variation of the frequency of occurrence and intensity of upwelling events based on the analyzed data is as it follows".

Figure 6. Maybe used dashed lines for the linear fits to emphasize the differences? Provide a correlation coefficient between CUI and CWS?

Response: We added the regression lines and mention the correlation coefficients for both sets of data (northern and southern coastal area). Nevertheless, we think that the linear correlation might not be the best model here.

L466. You mean the annual 'average values'. When using average and mean, please specify the period.

Response: Yes, the seasonal average values are meant here (since we analyzed the data from May to September). It is mentioned in the preceding sentence.

L471. 'over the all'. Remove 'the'.

Response: deleted.

L472-L474. 'This estimate respectively'. I am not sure what you mean with this sentence. How do 8.8 days and mean stress values relate?

Response: First, an average value of the cumulative wind stress for one upwelling event was found; just as an arithmetic mean for 17 events along the northern coast ($0.71 \text{ N m}^{-2} \text{ day}$) and 16 events along the southern coast ($-0.44 \text{ N m}^{-2} \text{ day}$). An average of these values is $0.135 \text{ N m}^{-2} \text{ day}$. If you divide it with the average duration of an upwelling event of 8.8 days, then an estimate of the wind stress is obtained as 0.015 N m^{-2} .

L474-L477. This is not clear either. The difference between the impulses is comparable to the average wind stress? Specify the difference. $0.71 - -0.44$? Or $0.71 + -0.44 = 0.27 \text{ N/m}^2$? The mean would be 0.13 N/m^2 (which is equally far removed from 0.71 and -0.44). This is 10 times larger than the mean of 0.015 N/m^2 .

Response: See the response to the previous comment. The units for the cumulative wind stress and average wind stress are different: the former has the units $[\text{N m}^{-2} \text{ day}]$ and the latter $[\text{N m}^{-2}]$. Thus, a cumulative wind stress of $0.135 [\text{N m}^{-2} \text{ day}]$ for an 8.8 days long event corresponds to an average wind stress of $0.135 [\text{N m}^{-2} \text{ day}] / 8.8 [\text{day}] = 0.015 [\text{N m}^{-2}]$.

L481-L484. Please explain the connection between daily measurements and the inertial period. This sentence is not clear. What is the link between this sentence and the rest of this paragraph that shows some examples of T and S for upwelling profiles?

Response: Since it creates some confusions, we deleted the sentence. The idea here was to explain why we did not analyze the temporal evolution of the upwelling events. We tried to analyze the temporal evolution of upwelling events but discovered that the changes during the initiation phase were very fast (one could need a few profiles during an inertial period of about 14 hours). Instead, we analyzed the shape when the upwelling was at its maximum extent/intensity.

L530-532. ‘not enough attention’. I think the installers know the fallacies, but you have to work with the ferry infrastructure. Changing this for the purpose of measurements is very costly. I suggest you remove this point.

Response: We do not agree and suggest to keep the sentence. It does not need costly investments; just the operators have to be aware that the water flow from the intake place to the sensors could take time. It is not an issue when the intake is very close to the sensors. However, we know the systems (similar to the one that we use) where this point is not considered at all and thus, the data are not correctly georeferenced.

L546. “We suggest that such coordinate correction procedure should be used in all Ferrybox systems”. I suggest you remove this point too. My experience is that these corrections are made to get the best georeferenced data (I certainly did that) – since everybody wants the best data. I think this point should not be one of the main conclusion of this paper. You should mention the most important findings first.

Response: It is deleted. At the same time, we suggest to keep a sentence above (see the Response to the previous comment).

L570. What are ‘those values’

Response: The words “those values” are replaced by “the values obtained from the remote sensing data”.

L583-585. Please explain the physics behind these reasons. Why are a deeper TC and topography reasons that explains the 0.71 vs -0.44 N/m² difference?

Response: We referred to the previous publications where the physics has been explained. However, we included an additional reference and some sentences to explain it in more detail. The Gulf of Finland is not a strait, but it is an estuary, which is closed at one end (eastern end). It is well known that the prevailing winds from the southwest and the freshwater discharge at the eastern end together with the Coriolis force result in a cyclonic circulation pattern in the gulf surface layer and associated deeper position of the thermocline in the northern part of the gulf. Note, that the prevailing wind is from the southwest, but the thermocline has a deeper position in the northern part of the gulf. If on the background of such distribution pattern, the up-estuary wind impulse occurs it can cause an upwelling along the northern coast. However, since in general, the thermocline is deeper near the northern coast the wind impulse needed should be stronger here than at the opposite coast. In addition, stronger up-estuary southwesterly winds, on the one hand, cause upwelling along the northern coast, but on the other hand downwelling in the whole gulf (which results in a weaker upwelling than the wind forcing suggests). In the case of down-estuary winds, a general upwelling in the whole gulf supports the coastal upwelling along the southern coast.

L585-587. “However, one could suggest that the thermohaline structure of the Gulf of Finland is adapted to the general prevalence of westerly-south-westerly winds.” Ok this is not clear to me. How can there be a structure (TC slope) if the mean wind stress is almost zero (0.015 N/m²)? If it was 0.135 N/m² your argument would be stronger. Please explain this better.

Response: We rephrased the paragraph and give some explanations here. It is well known that such average wind stress (since it is directed up-estuary) and the freshwater discharge at the closed end of this east-west-oriented estuary (together with the Coriolis force) cause general (residual) cyclonic circulation in the Gulf of Finland (see e.g. Alenius et al. 1998). Such circulation, if one applies the geostrophic balance, yields in higher sea level and deeper thermocline at the northern part of the gulf (it has been demonstrated by modeling studies; e.g. see Andrejev et al., 2004). We also refer to an analysis of cross-gulf CTD sections in the summers 2006-2013, presented in a submitted manuscript by Liblik and Lips (2016), where it is also shown based on in situ data that in general the thermocline has a deeper position in the northern part of the gulf although the southwesterly winds prevail. The mean wind stress is low, but it is a long-term (climatic) average, and this wind stress contributes to the general circulation and thermohaline structure. Please also note that the wind stress referred here is from the southwest (but the thermocline is on average deeper in the northern part).

L588-591. “This suggestion ... gulf” After rereading this sentence several times I still do not know what the authors want to say here. What does the comparison show?

Response: We rewrote this paragraph to be more precise in formulations. This particular sentence is written now as: “This suggestion is supported by the comparison of the lowest cumulative wind stress values, which have initiated upwelling events in 2007-2013 near the opposite coasts of the gulf (see Fig. 6)”.

L590. “for the all”. English!

Response: Corrected.

L598. Please specify the general circulation scheme.

Response: It is explained in the Introduction as: “The long-term residual circulation in the surface layer of the gulf is characterized by a relatively low speed and by a cyclonic pattern. The saltier water of the northern Baltic Proper flows into the gulf along the Estonian (southern) coast and the gulf water, which is less saline due to the large freshwater inflow at the eastern end of the gulf (the Neva River), flows out along the Finnish (northern) coast.” Here, a reference is given to the paper by Andrejev et al. (2004), where the authors showed that the outflow in accordance with the general circulation scheme occurs in the northern part of the gulf at some distance from the shore.

L616. “Since often the wind conditions were quite variable before the upwelling events, it was not possible to suggest any quantitative criterion for wind forcing generating one or the other type of temperature distribution.” If this is the case, what is the point of showing Figure 8. I suggest you remove this figure.

Response: We prefer to keep Fig. 8, which is relevant to one of our discussion points. The text is reformulated. As the main change, we divided the explanation of the occurrence of the two types of temperature distribution into two parts. First, regarding weaker and shorter term upwelling events, we argue that one reason of occurrence of gradual decrease type of upwelling events could be related to the strength of the wind forcing. This explanation is illustrated by Fig. 8.

The other explanation is related to the strong upwelling events, for which the generation of filaments and squirts due to the baroclinic instability of the upwelling jet is more probable near the northern coast where the bottom slope is twice less than near the southern coast. We included two more relevant references in the manuscript. These explanations are at the moment just suggestions; we prefer to mention them but not go into very detail analysis in this paper, which already have its main results related to the different reaction of the southern and northern

upwelling events to the wind forcing. We mention the finding of the two types of upwelling events in the concluding sentences, but we do not describe the possible explanations as the main conclusions of the present study.

L625. ‘could be related’. Could the shear in windstress play a role? Do you have references that show that (sub)mesoscale variability (you mean eddies?) causes the steep fronts? So it is not really related to upwelling?

Response: It is the opposite. We suggest that if there exist a strong (steep) front than it is a major manifestation of a mesoscale dynamical feature – the upwelling front. In contrary, when the variability at scales of a few kilometers exists, no steep upwelling front is observed. Thus, such spatial variability in temperature distribution is suggested to be caused by the meso- and sub-mesoscale features (filaments and squirts).

L626. “which are made visible if due to the slightly lower forcing the mesoscale dynamics do not fully dominate.” This is not clear. Explain better.

Response: We suggest that if the wind forcing is strong enough to initiate an upwelling event but not as strong as needed to retain the mesoscale frontal dynamics, the mesoscale and the sub-mesoscale ageostrophic processes (e.g. cold/warm squirts, filaments) develop and shape the horizontal temperature distribution.

L632-634. ‘Thus waters’ Again some more explanation is needed. Where does the deepening occur? On the north shore?

Response: We hope, we have explained it now in several places throughout the manuscript as well as in the present response to the comments.

L642. Why not make this in a separate conclusion chapter?

Response: Thank you. It is done in the revised manuscript.

L654. “deviation from the average”. The mean is 0.015 N/m². So I do not think there is a strong horizontal thermocline slope associated with this value?

Response: It is enough to influence the general circulation in the Gulf of Finland (see our explanations above and e.g. Alenius et al., 1998; Andrejev et al., 2004; etc.). Please, pay attention that the prevailing wind is from the southwest, but the thermocline has a deeper position in the northern part of the gulf.

L658-661. Please specify what sub-mesoscale motions and how do they interact with the upwelling?

Response: We do not think it is a right place to discuss the findings in the concluding paragraph. See also the response above (regarding the spatial variability at sub-mesoscale).

1 **Upwelling characteristics in the Gulf of Finland (Baltic Sea) as revealed by Ferrybox**
2 **measurements in 2007-2013**

3

4 Villu Kikas, Urmas Lips

5

6 Marine Systems Institute at Tallinn University of Technology

7 Akadeemia tee 15a, 12618 Tallinn, Estonia

8 Tel: +3726204315, Fax: +3726204301

9 e-mail: villu.kikas@msi.ttu.ee

10

11 **Abstract.** Ferrybox measurements are carried out between Tallinn and Helsinki in the Gulf of
12 Finland (Baltic Sea) on a regular basis since 1997. The system measures autonomously water
13 temperature, salinity, chlorophyll *a* fluorescence and turbidity and takes water samples for
14 further analyses at a predefined time interval. We aimed to show how the Ferrybox technology
15 could be used to study the coastal upwelling events in the Gulf of Finland. Based on the
16 introduced upwelling index and related criterion, 33 coastal upwelling events were identified in
17 May-September 2007-2013. The number of events, as well as the frequency of their occurrence
18 and intensity expressed as a sum of daily average temperature deviations in the 20-km wide
19 coastal area, were almost equal near the northern and southern coast. ~~It is shown~~
20 ~~that~~ Nevertheless, the wind impulse, which was needed to generate upwelling events of similar
21 intensity, differed between the two coastal areas. It is suggested that the general thermohaline
22 structure adapted to the prevailing forcing and the estuarine character of the basin weaken the
23 upwelling created by the westerly-southwesterly (up-estuary) winds and strengthen the upwelling
24 created by the easterly-northeasterly (down-estuary) winds. Two types of upwelling events were
25 identified – one characterized by a strong temperature front and the other revealing gradual
26 decrease of temperature from the open sea to the coastal area with maximum temperature
27 deviation close to the shore.

28

29 **Keywords:** Ferrybox, coastal upwelling, upwelling index, cumulative wind stress, Gulf of
30 Finland

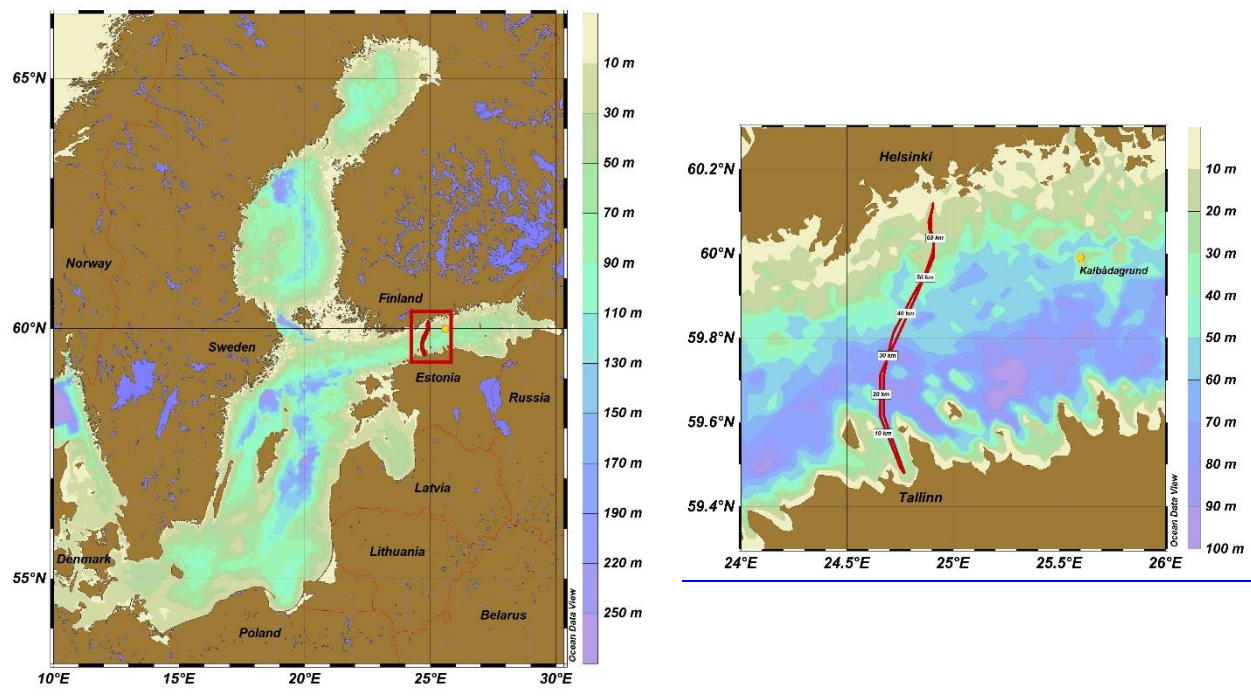
31

33 **1. INTRODUCTION**

34

35 Unattended monitoring of marine environment using ships of opportunity has been implemented
36 in many regions of the World Ocean (e.g. Paerl et al., 2009; Hardman-Mountford et al., 2008)
37 including the Baltic Sea and the Gulf of Finland (Rantajarvi, 2003). The measurement systems
38 installed on board commercial ferries or other ships are called “Ferryboxes” and they consist of
39 various sensors, devices creating water flow through the sensors and software packages
40 controlling the system and managing the data. The commonly used Ferryboxes measure
41 temperature, salinity, and chlorophyll *a* fluorescence in the seawater pumped through the system
42 from the surface layer along the ship track. First trials of using ships of opportunity for
43 environmental monitoring in the Gulf of Finland were made by Estonian and Finnish scientists
44 between Tallinn and Helsinki in 1990-1991 (Rantajarvi, 2003). Regular Ferrybox measurements
45 along this route were started in 1997 while the longest data series of Ferrybox measurements
46 (since 1993) is available along the ferry route Helsinki-Travemünde (Petersen, 2014).

47



48

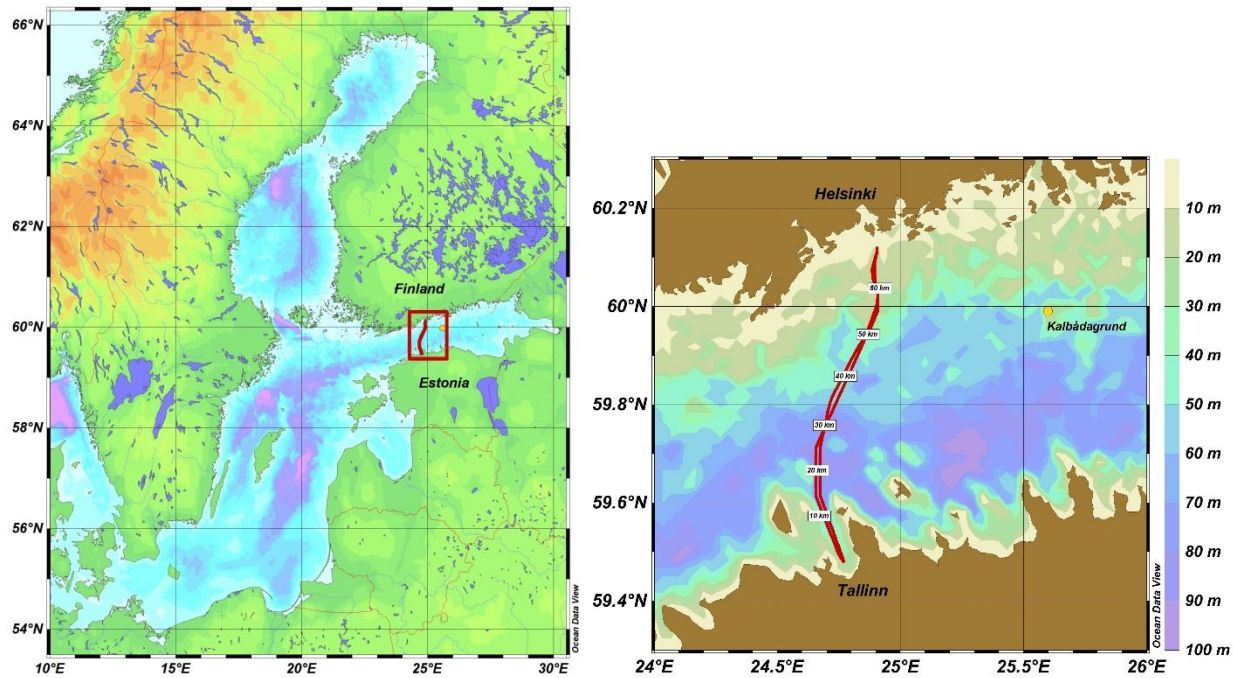


Figure 1. Map of the Baltic Sea (a) and the study area (b) with the Ferrybox transect and Kalbadagrund meteorological station.

49

50

51

52 The Gulf of Finland (GoF) lies in the northeastern part of the Baltic Sea (Fig. 1). It is an
 53 elongated basin with a length of about 400 km and a maximum width of 135 km (Alenius et al.,
 54 1998). The long-term residual circulation in the surface layer of the gulf is characterized by a
 55 relatively low speed and by a cyclonic pattern. The saltier water of the northern Baltic Proper
 56 flows into the gulf along the Estonian (southern) coast and the gulf water, which is less saline
 57 due to the large freshwater inflow at the eastern end of the gulf (the Neva River), flows out along
 58 the Finnish (northern) coast. The circulation is more complex at time scales from days to weeks
 59 mainly due to the variable wind forcing. A variety of mesoscale processes/features (fronts,
 60 eddies, upwelling/downwelling), which significantly affect the biological production, retention,
 61 and transport, have been observed in the Gulf of Finland (e.g. Talpsepp et al., 1994; Pavelson et
 62 al., 1997; Lips et al., 2009).

63

64 The vertical stratification in the gulf is characterized by a quasi-permanent halocline at the
 65 depths of 60-80 m, and a seasonal thermocline, which forms in spring-summer at the depths of
 66 10-20 m (e.g. Liblik and Lips, 2011). While high concentrations of dissolved inorganic nitrogen
 67 (DIN) and phosphorus (DIP) are observed in winter, the concentrations of DIN and DIP are
 68 usually below the detection limit in summer in the upper mixed layer but still high just below the

69 seasonal thermocline. In general, the most prominent features of the seasonal dynamics of
70 phytoplankton in the Gulf of Finland are the spring bloom in April-May dominated by
71 dinoflagellates/diatoms and the late summer bloom in July (or late June to mid-August)
72 dominated by cyanobacteria (Kononen et al., 1996). However, the variations in bloom intensities
73 and their spatial distributions are very high over the years and within the season that is often
74 related to the physical forcing and especially to the mesoscale processes, including upwelling
75 events (Lips and Lips, 2008; Vahtera et al., 2005).

76

77 Dynamics and characteristics of upwelling events have been studied in the Gulf of Finland based
78 on in-situ measurements (e.g. Haapala, 1994), remote sensing (e.g. Uiboupin and Laanemets,
79 2009) and modeling (e.g. Myrberg and Andrejev, 2003). Most prominent upwelling events that
80 were captured by measurements are an event along the northern coast in July 1999 (Vahtera et
81 al., 2005) and an event along the southern coast in August 2006 (Lips et al., 2009). The
82 following characteristic features of upwelling events in the Gulf of Finland are suggested:

83

- 84 1) the Finnish coastal sea in the north-western GoF is one of the main upwelling areas in the
85 Baltic Sea (Myrberg and Andrejev, 2003) where upwelling frequency in May-September
86 1990-2009 has been up to 15% (Lehmann et al., 2012); almost the same upwelling
87 frequency is suggested by the latter authors for the central GoF along the Estonian
88 (southern) coast;
- 89 2) mean upwelling area detected on the basis of 147 maps during the period of 2000-2009
90 was 5642 km² (19% of the GoF surface area) along the northern coast and 3917 km²
91 (13% of the GoF surface area) along the southern coast (Uiboupin and Laanemets, 2015),
92 while the largest area covered by the upwelling water was identified as 12140 km² (data
93 from 2000-2006; Uiboupin and Laanemets, 2009); the authors' estimate of the mean
94 cross-shore extent of upwelling area was 20-30 km off the northern coast and varied
95 between 7 and 20 km off the southern coast;
- 96 3) the intensity of upwelling events depends on the values of cumulative upwelling-
97 favorable wind stress and strength of vertical stratification; Haapala (1994) suggested that
98 at least 60 h long wind event has to exist to create an upwelling event; based on the wind
99 data analysis from 2000-2005 and taking the threshold value for cumulative wind stress

100 of 0.1 N m⁻² d, on average, about 2 upwelling events should appear off the southern coast
101 and 4 events off the northern coast (Uiboupin and Laanemets, 2009);

102 4) it is suggested that the difference in topography off the southern and northern coast of the
103 GoF results in differing upwelling dynamics along the opposite coasts – in case of similar
104 wind stress (but in opposite directions) the transport of waters from deeper layers starts
105 earlier and is larger along the southern coast (Väli et al., 2011).

106
107 The motivation of the present paper is to show how the Ferrybox technology can be used to
108 study mesoscale processes, especially coastal upwelling events in the Gulf of Finland. We
109 describe the approach, its advantages and limits, and present statistical characteristics of
110 upwelling events on the basis of data collected in 2007-2013. The main aim is to relate the
111 observed variability and dynamics of upwelling events to the atmospheric forcing, ~~and~~ reveal the
112 differences in upwelling behavior in the two ~~(the one opposite to the other)~~ coastal areas and
113 suggest an alternative physical explanation of the found differences by taking into account the
114 prevailing forcing and estuarine character of the basin.

115
116

117 2. THE MEASUREMENT SYSTEM AND METHODS

118

119 2.1. Ferrybox system

120

121 Temperature (T), salinity (S), chlorophyll *a* fluorescence and turbidity data and water samples
122 for nutrients and phytoplankton chlorophyll *a* (Chl *a*), species composition and biomass analyses
123 are collected unattended on passenger ferries, traveling between Tallinn and Helsinki (Fig. 1)
124 since 1997. Due to the internal arrangements of the ferry company Tallink Silja and its
125 predecessors, several ships were used as the platforms for Ferrybox measurements, which also
126 differ regarding water intake features. A flow-through system from 4H-Jena, Germany with the
127 water intake attached to the sea chest of the ferry is in use since 2006. The water enters the sea
128 chest through a grating with a total surface area of 0.84 m² located at about 4 m depth below the
129 waterline. The water flow from the sea chest into the system is forced by the hydrostatic pressure
130 since the Ferrybox is located on the lower deck about 3 meters below the waterline. To restrict

131 larger particles to get into the measurement system a mud filter (pore size 1 mm) is used close to
132 the water intake. Before the sensors, a debubbler is installed to avoid air bubbles to affect the
133 measurements of conductivity, turbidity and Chl *a* fluorescence. The flow rate through the
134 sensors is stabilized by an internal pump, which is controlled by a pressure sensor in the system.
135 Water samples are taken by a sampling device (Hach Sigma 900 MAX) whereas the water is
136 pumped from the debubbler into the bottles using an internal pump of the water sampler.

137
138 For temperature measurements, a PT100 temperature sensor is used that is installed close to the
139 water intake to diminish the effect of warming of water while flowing through the tubes onboard.
140 The sensor has a measuring range from -2 to +40 °C and accuracy of ±0.1% of the range, thus
141 0.04 °C. For salinity measurements an FSI Excell thermosalinograph (temperature and
142 conductivity meter) and for Chl *a* fluorescence and turbidity measurements a SCUFA
143 submersible fluorometer (Turner Designs) with a flow-through cap is used. The system starts the
144 measurements and data recording when the ferry is away from the harbor more than a predefined
145 distance of 0.7 nautical miles (controlled by a GPS device in the system) and stops when it is
146 closer than this distance to avoid sediments getting into the system. The data are recorded during
147 every crossing (twice a day) every 20 seconds that corresponds to a horizontal resolution of
148 approximately 160 m.

149

150 **2.2. Quality assurance and pre-processing of data**

151

152 The sensors have been calibrated at the factory before the installation and if necessary sent for an
153 additional laboratory calibration. Since the system contains two temperature sensors, the
154 performance of them is routinely followed by a comparison of data acquired from the sensors.
155 The quality of thermosalinograph data is guaranteed by taking a series of water samples (14-17
156 samples) and analyzing them using a high-precision salinometer AUTOSAL 2-4 times a year.
157 The analyses have shown, that a correction of 0.08 (units in Practical Salinity Scale; the value
158 has been stable over the years) must be added to the recorded salinity. While the raw salinity is
159 recorded in units according to the Practical Salinity Scale 1978, the results on salinity
160 distribution and variability are given later in this paper in g kg^{-1} (Sections 3 and 4). Particular

161 care is taken to calibrate the SCUFA fluorometer; however, since we do not use the fluorometer
162 data in this study the used routine is not described here.

163
164 | The data acquired by the Ferrybox system ~~are~~ recorded with a time step of 20 s ~~and are~~ stored in
165 an onboard terminal. To synchronize the measurements performed by the sensors having
166 different sampling frequencies and GPS, the acquired data within every 19 s interval are
167 averaged and recorded as measurements at every 20th second. The data are automatically
168 delivered to the on-shore FTP-server once a day when the ferry is in the harbor using a GSM
169 connection. The performance of the system is validated by the control parameters, such as the
170 flow rate and pressure in the system, and the data are checked for unrealistic values against the
171 criteria set for every parameter on the basis of known natural variation of them in the Gulf of
172 Finland.

173
174 One of the procedures, which has to be carried out when using the Ferrybox data, is the shifting
175 of data points to the actual positions of the water intake. The problem arises since the coordinates
176 attached to a data record correspond to the location of the ferry at the time of measurement, but
177 the water is taken in earlier at a different position. Since various systems of water intake are
178 applied, this procedure is unique for each combination of a Ferrybox and a ferry. As described
179 above, in our design the seawater enters first a relatively large sea chest and the flushing through
180 time of it is unknown. While the water flows through the sea chest and into the tubes and
181 debubbler with a flow rate of 12-15 l min⁻¹, the ferry moves on at an average speed of 16 knots.
182 We solved the problem of position correction taking into account the advantage of having two
183 crossings a day.

184
185 Analysis of data from forth and backward journeys allowed us to introduce a position correction
186 procedure – the best result is achieved by shifting the measured data points against the GPS time
187 for 3-4 minutes depending on the ferry and exact intake installation. This relatively long period is
188 obviously related to the water exchange in the sea chest. Due to an almost constant cruising
189 speed of the ferry outside the harbor areas, the applied procedure gives acceptable results. The
190 comparison of data from Tallinn to Helsinki and back from Helsinki to Tallinn obtained on the

191 same day is one of the used quality assurance procedures – the profiles containing unexpected
192 deviations are marked by a quality flag indicating a possible quality problem.

193

194 **2.3. Data and calculation methods**

195

196 Temperature and salinity data collected along the ferry line Tallinn-Helsinki from May to
197 September in 2007-2013 are used for analysis purposes. In 2008, the system on board the
198 passenger ferry “Galaxy” was in use until 13 July and the measurements started again on 13
199 August when the system was installed on board the ferry “Baltic Princess”. However, due to
200 some technical problems, the regular measurements were successful from 2 September 2008. A
201 failure of the system occurred late August 2012 and, therefore, the data are not available from 29
202 August until the end of September 2012. In early 2013, the next ferry (“Silja Europa”) came to
203 this line and the system was moved again causing a break in the measurements until 15 July
204 2013. The number of crossings with the full data coverage is given in Table 1. Four years –
205 2007, 2009, 2010 and 2011 – were the years with almost complete data coverage while most of
206 the data were not available in the second half of July and August 2008, in September 2012 and in
207 May, June and [the](#) first half of July 2013. Thus, the data from all months from May to September
208 were analyzed at least from six years in 2007-2013.

209

210 Collected raw data were preliminarily processed, including shifting of measurements as
211 described in Section 2.2, quality checked and stored in the database. This data set was used to
212 draw the maps of temporal variations of horizontal distributions of T and S for all studied years
213 (Fig. 2). A step (cell width) of 0.5 km along the south-north oriented line was used to transform
214 the data set from the matrix with [a](#) constant time step into the matrix with a constant spatial
215 resolution. The fixed south-north orientation was applied to eliminate the influence of
216 differences in orientation of the ship track in the southern, central and northern parts of the route
217 (see Fig. 1) and of possible deviations from the ordinary route. As a result, the extent of the
218 upwelling area is presented below in the south-north direction, and a coefficient has to be applied
219 to convert these values to the upwelling extent in the cross-shore direction (as the cosine of the
220 angle between the south-north direction and a perpendicular line to the shore – approximately 20
221 degrees).

222

223 An upwelling index was introduced in the coastal area off the southern coast (UI_S) and off the
224 northern coast (UI_N). For each crossing, the average water temperature and horizontal profile of
225 temperature deviations from the average were found. The upwelling index was calculated as a
226 sum of negative temperature deviations in the 20-km coastal areas as:

$$227 \quad UI_S = \sum_{\Delta T_i < 0}^{i=1 \dots 40} |\Delta T_i| \quad \text{and} \quad UI_N = \sum_{\Delta T_i < 0}^{i=101 \dots 140} |\Delta T_i| \quad (1)$$

228 where ΔT_i is the temperature deviation at 0.5-km cell i from the average temperature of the
229 crossing. The width of 20 km was selected on the basis of the analysis of all available
230 temperature data from Tallinn-Helsinki ferry line in 2007-2013 (see Section 3.1 for details). The
231 daily indexes were obtained by averaging the two upwelling indexes from a single day (from
232 forth and backward journey of the ferry). The cumulative upwelling index (CUI) can be
233 calculated by summing up upwelling index values for certain periods. The obtained CUI values
234 were divided by 40, which is the number of data cells in the 20-km wide coastal area, to keep the
235 meaning of CUI as the sum of average negative temperature deviations, having a unit of [$^{\circ}\text{C}$
236 day]:

$$237 \quad CUI_S(n1 \dots n2) = \sum_{j=n1}^{j=n2} \left(\frac{1}{40} UI_{Sj} \right) \quad \text{and} \quad CUI_N(n1 \dots n2) = \sum_{j=n1}^{j=n2} \left(\frac{1}{40} UI_{Nj} \right) \quad (2)$$

238

239 where $n1$ and $n2$ are the start and the end day number of the selected period, for which the
240 cumulative upwelling index is calculated, and UI_{Sj} and UI_{Nj} are the upwelling indexes at day j off
241 the southern and northern coast, respectively. This approach of the CUI calculation is similar to
242 those used previously in the studies of upwelling events and their influence on the phytoplankton
243 dynamics in the Gulf of Finland (see e.g. Lips and Lips, 2008; Myrberg et al., 2008).

244

245 An upwelling event can be characterized by the cumulative upwelling index whereas the first and
246 the last day of the event can be defined as the start and end of the period when the upwelling
247 index (UI_N or UI_S) exceeded a certain threshold value. We have defined this threshold value as
248 40 $^{\circ}\text{C}$, which corresponds e.g. to a 20-km wide upwelling with an average negative temperature
249 deviation of 1 $^{\circ}\text{C}$. This choice is explained in more detail in Section 3.2. ~~Although the precision
250 of the temperature sensor is better than its accuracy, we estimated the uncertainty of the
251 calculated index values based on the absolute accuracy of PT100.~~ The accuracy of the

252 | temperature ~~measurements~~ sensor of 0.04 °C gives a maximum uncertainty of 1.6 °C in the
253 | upwelling index estimates (since it is a sum of 40 temperature values – 40*0.04 °C). ~~It is 25~~
254 | ~~times less than the selected threshold for the upwelling detection (40 °C) and a maximum~~
255 | ~~uncertainty of 0.4 °C day in the cumulative upwelling index estimates (considering a 10 day~~
256 | ~~upwelling event).~~

257

258 | Wind data were obtained from the HIRLAM (High-Resolution Limited Area Model) version of
259 | the Estonian Meteorological and Hydrological Institute with the spatial resolution of 11 km and
260 | the time interval of 3 h (Väli, 2011; Männik and Merilain, 2007). Model data point close to
261 | Kalbådagrund, where also a meteorological weather station is located (Finnish Meteorological
262 | Institute), was chosen to represent the wind conditions in the study area. The data from
263 | Kalbådagrund weather station or the closest HIRLAM model point have also been used in the
264 | earlier studies describing wind conditions of coastal upwellings in the Gulf of Finland (Lips et al.,
265 | 2008a; Uiboupin and Laanemets, 2009). According to Keevallik and Soomere (2010), the
266 | HIRLAM ~~model output~~ matches well with the observations at Kalbådagrund (the wind is
267 | measured at 32 m) measured wind speed as well wind directions, whereas although the modeled to
268 | obtain the wind direction (at 10 m height) is turned by 20° counter-clockwise from the measured
269 | ~~wind direction at Kalbådagrund (measured at 32 m) is advised to turn by 20° counter clockwise.~~

270

271 | Wind stress (in N m⁻²) is calculated for the wind component along the axis of the Gulf of
272 | Finland, which corresponds to the direction turned by 70 degrees clockwise from the north
273 | direction, as:

$$274 \quad \tau_{70} = C_D \rho_a |U| U_{70} \quad (3)$$

275 | where U is the wind speed (in m s⁻¹), U_{70} is its component in the along-gulf direction, C_D is the
276 | drag coefficient (a value of $1.2 \cdot 10^{-3}$ was chosen in the present study), and ρ_a is the air density
277 | (1.2 kg m^{-3}). Accordingly, positive values of the wind stress should initiate southward Ekman
278 | transport in the surface layer and vice versa. The cumulative wind stress (in N m⁻² day) was
279 | calculated based on daily averages of wind stress. If the cumulative wind stress is large enough,
280 | upwelling events occur along the northern coast in case of the positive wind stress and along the
281 | southern coast in case of the negative wind stress.

282

283 **3. RESULTS**

284

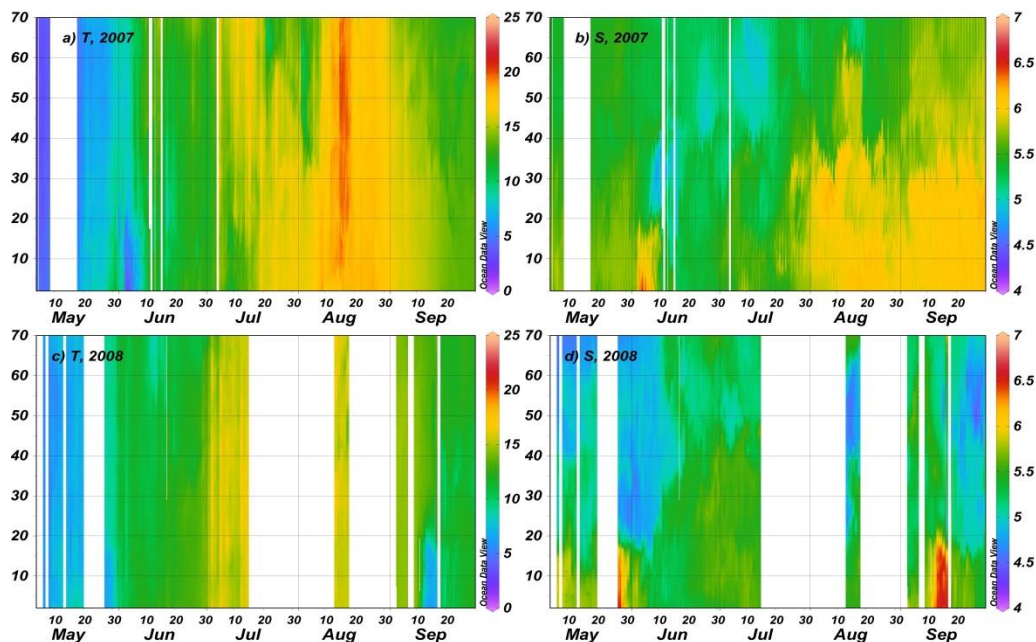
285 **3.1 General variability and distribution patterns**

286

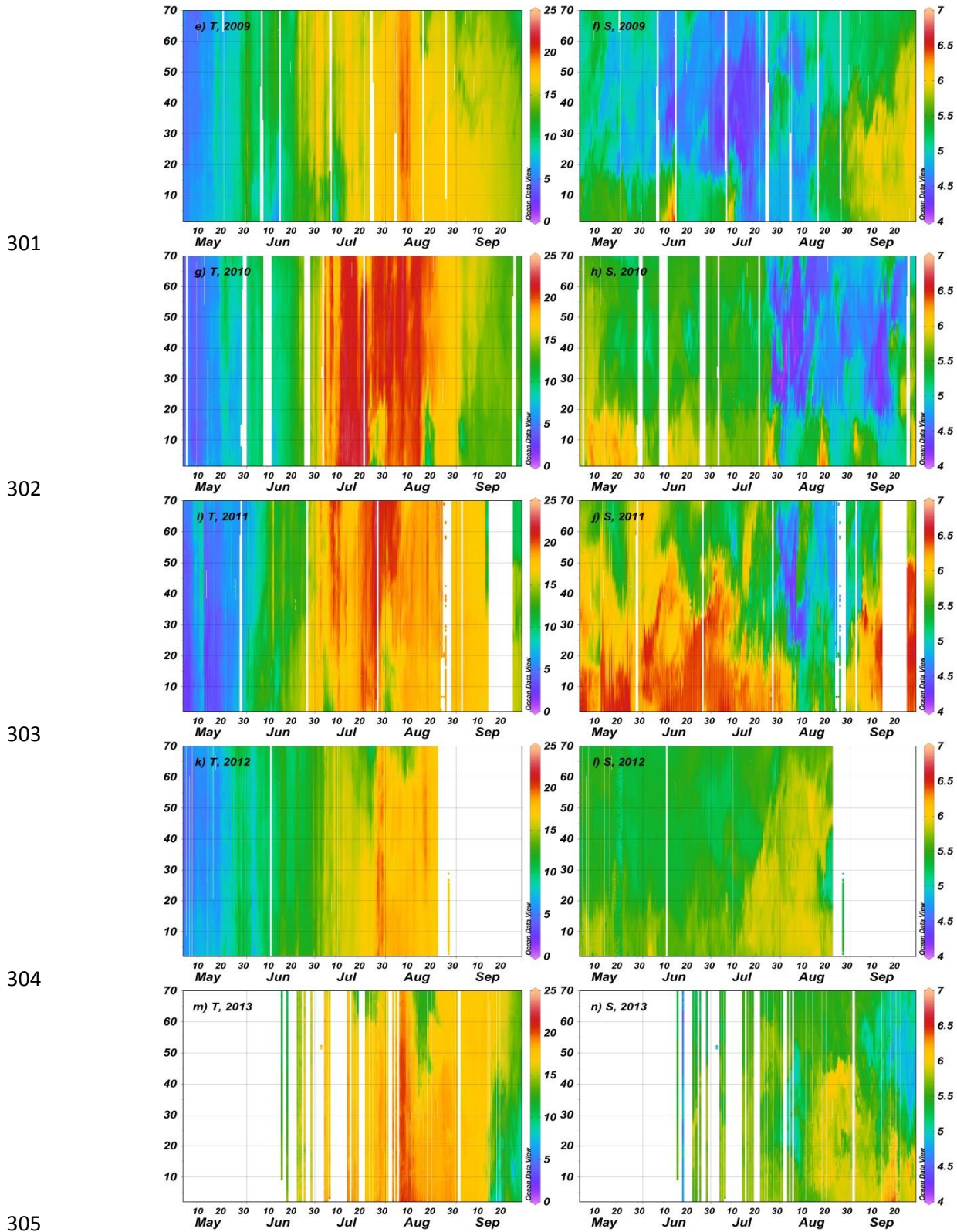
287 The typical ~~seasonal trend~~ course of the surface layer temperature in the Gulf of Finland ~~in the~~
288 ~~warm season~~ is characterized by temperature about 5 °C at the beginning of May, a maximum >
289 20 °C in late July – early August and a drop below 15 °C in late September. Within the analyzed
290 years 2007-2013, the surface layer temperature was the highest in summer 2010 (Fig. 2). ~~When~~
291 ~~the period when with the average along-transect surface-layer~~ temperature ~~≥~~ exceeded 20 °C was
292 ~~the longest in 2010 35 days and 2011 while the periods with water temperature > 20 °C were very~~
293 ~~short (only a few days) in the other years~~. On the background of seasonal ~~course~~ trend and
294 simultaneous shorter-term increases or decreases of temperature over the whole study transect,
295 the periods with distinctly lower temperature were observed off the northern or southern shore.
296 Such situations are related to the coastal upwelling events – their characteristic time scale was
297 several days to 1-2 weeks, and they extended towards the open sea by 15-20 km (Fig. 2).

298

299



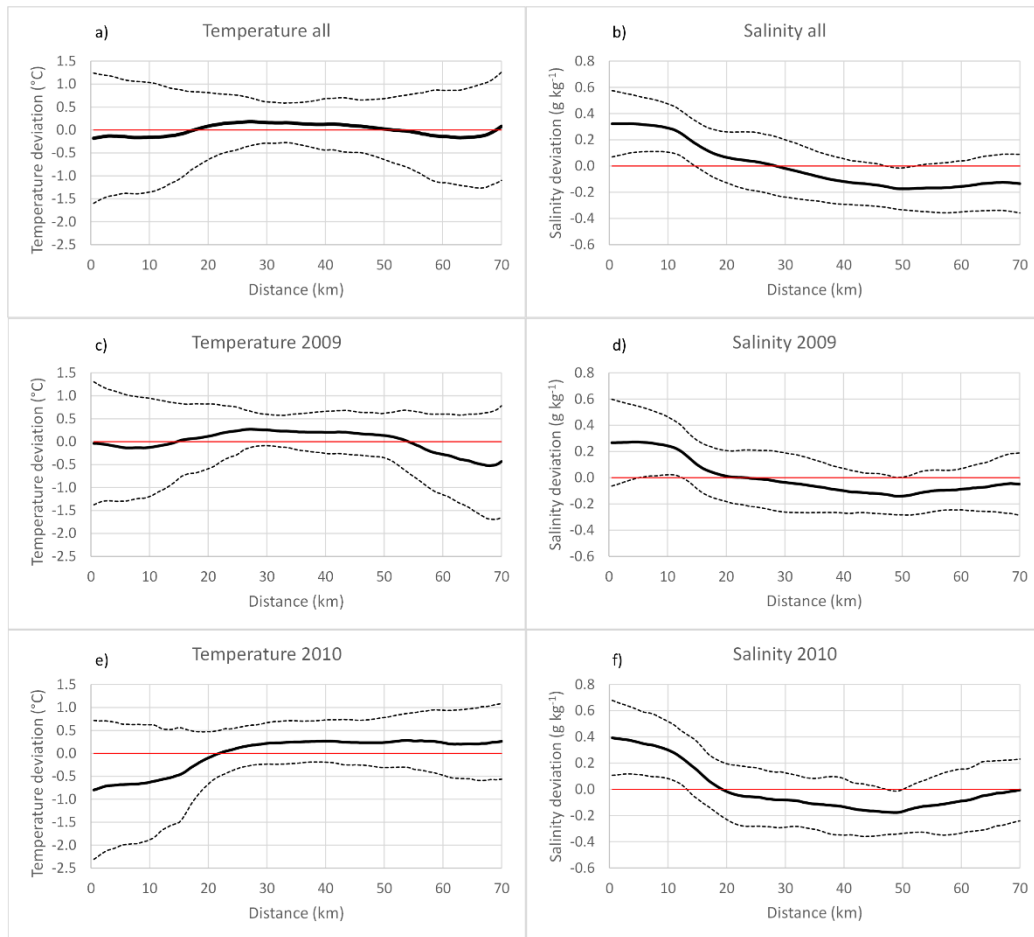
300



306 Figure 2. Temporal changes in temperature (in °C) and salinity (in g kg⁻¹) distributions between Tallinn and Helsinki from 1 May to 30
 307 September in 2007 (a, b), 2008 (c, d), 2009, (e, f), 2010 (g, h), 2011 (i, j), 2012 (k, l) and 2013 (m, n); y-axis shows the distance from the Tallinn
 308 Bay (latitude 59.48 N) in km along the meridional transect.

309

310 Inter-annual variations of the surface layer salinity in 2007-2013 were high with the highest
311 salinity in 2011 and the lowest in 2009. The surface layer salinity exceeded 6.5 g kg^{-1} for a
312 longer period only in 2011 in the southern half of the study transect (Fig. 2j) and for shorter
313 periods of several days in case of coastal upwelling events off the southern shore (e.g. Figs. 2b
314 and 2d). Note that in the case of coastal upwelling events seen in the temperature distributions
315 off the northern coast, a simultaneous increase in salinity was not well visible. As a rule, the
316 surface layer salinity was higher near the southern coast than that near the northern coast.
317 However, often the lowest salinity was measured in the middle of the transect – it means in the
318 | open sea areas (e.g. Figs. 2f and 2h). Seasonal ~~course~~-trend of salinity differed between the
319 studied years remarkably. While usually, the lowest surface layer salinity was observed in June-
320 July, in 2008, the salinity was the lowest in May, and in 2010 and 2011, it was the lowest in
321 August.



322

323

324 | **Figure 23.** Distributions of temperature (in °C) and salinity (in g kg^{-1}) deviations from the **daily**-transect mean value along the ferry route
 325 Tallinn-Helsinki for all measurements in May-September 2007-2013 (a, b), 2009 (c, d) and 2010 (e, f). Mean values for each 0.5-km cell (solid
 326 curves) and plus/minus RMSE (dashed curves) are shown; x-axis indicates the distance from the Tallinn Bay (latitude 59.48 N) in km along
 327 the meridional transect.

328

329 | The average temperature and salinity deviations [in May-September each year and for the entire](#)
 330 [study period](#), as well as their root mean square errors (RMSE), were calculated [in each 0.5-km](#)
 331 [cell](#). On average, the temperature deviations were close to zero along the entire study transect
 332 (Fig. 3a) – the absolute values of average deviation were six times less than estimated RMSE of
 333 temperature. Nevertheless, the surface layer temperature was slightly warmer in the open Gulf of
 334 Finland than ~~that~~ in approximately 20-km wide coastal areas (Fig. 3a). This result could be
 335 related to the coastal upwelling events. For instance, in 2009, when coastal upwelling events
 336 were observed off the both coasts, the average temperature deviations were negative near the
 337 both coasts (Fig. 3c). In 2010, when upwelling events occurred mostly off the southern coast, the

338 negative values of average temperature deviations were detected only in the southern part of the
339 transect (Fig. 3e).

340
341 It is remarkable that, on average, the variability of temperature deviations was much higher near
342 the coasts than in the central part of the study transect (Fig. 3a). In the case of upwelling events
343 off the southern coast and their absence off the northern coast (in 2010), this high variability of
344 temperature was concentrated only in the 20-km wide coastal area off the southern shore (Fig.
345 3e). Since the area of the high variability of temperature, which mostly could be related to the
346 upwelling activity, extended about 20 km from the shores, it was suggested to estimate the
347 intensity of upwelling events based on data from these 20-km wide coastal zones.

348
349 The average distribution of the surface layer salinity along the transect was characterized by
350 higher salinity values in the southern gulf and lower values in the northern gulf (Fig. 3b). The
351 salinity deviations were positive in the 28-km wide area off the southern coast (with clearly
352 higher salinity in the first 10 km) and negative along the rest of the study transect. However, the
353 minimum of the surface layer salinity was observed at about 20 km from the northern shore (or
354 at a distance of 50 km from the southern end of the study transect) almost in every year (Fig. 3b,
355 d, and f). The only exception was the year 2007 when the lowest salinity was observed on
356 average in the cell closest to the northern shore. The low salinity water at the distance of 50 km
357 indicates that, in summer, the outflow of the less saline Gulf of Finland surface waters occurs
358 mostly in the northern part of the open gulf. The spatial differences in variability of the surface
359 layer salinity were not so distinct than in variability of the surface layer temperature. One can
360 recognize slightly higher variability (RMSE) of the surface layer salinity in the coastal areas and
361 the southern part of the open gulf at the distance of 20-30 km.

362

363 **3.2 Upwelling characteristics**

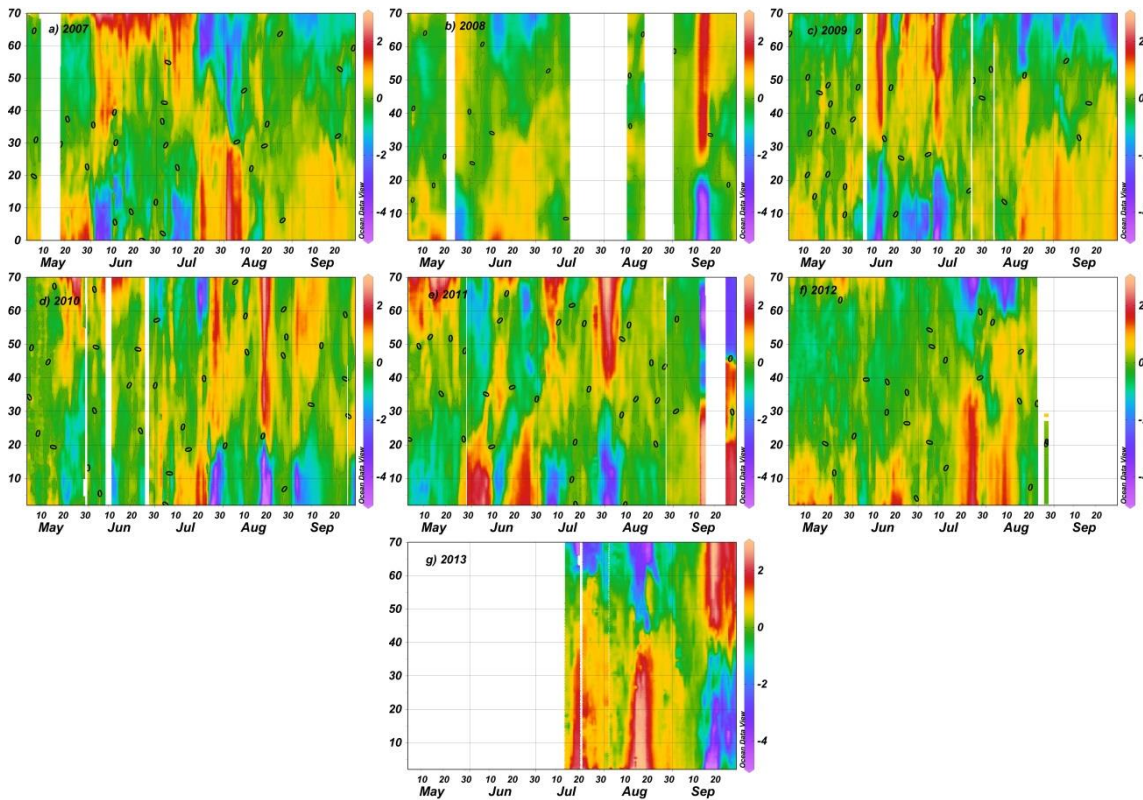
364

365 As it is seen on the maps of temperature deviations (Fig. 4), the years 2007 and 2009 had a
366 similar pattern – the upwelling events occurred off the southern coast in the first half of the
367 season and off the northern coast in the second half. In 2008, upwelling events were observed
368 near the southern coast in May and September, and they appeared near the northern coast in

369 June. The year 2010 was an exceptional year when the upwelling events occurred mostly along
 370 the southern coast. It was exceptional also because the sea surface temperature outside the
 371 upwelling waters was the highest among the studied summers. A sequence of consecutive
 372 upwelling events near the northern and southern coast was observed in 2011. Upwelling events
 373 occurred mostly off the northern coast in 2012 and 2013.

374

375



376

377

378 **Figure 4. Temporal changes in spatial distributions of temperature deviations (in °C) from the daily transect mean value between Tallinn and**
 379 **Helsinki from 1 May to 30 September in 2007 (a), 2008 (b), 2009, (c), 2010 e), 2011 (f), 2012 (g) and 2013 (h); y-axis shows the distance from**
 380 **the Tallinn Bay (latitude 59.48 N) in km along the meridional transect.**

381

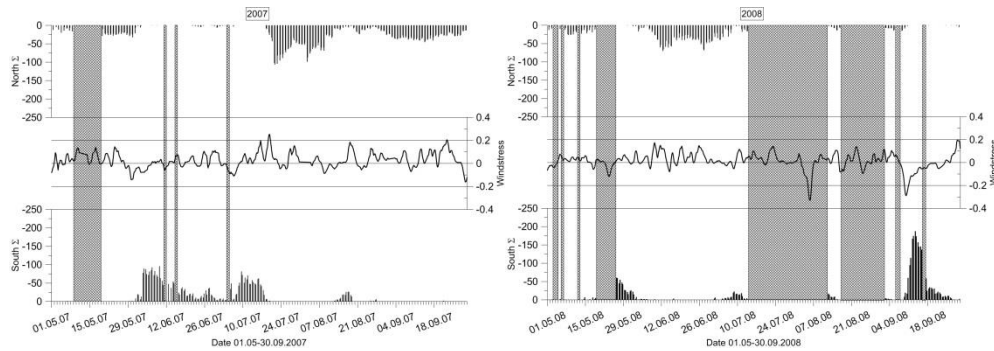
382 | We selected a criterion to detect whether an upwelling event occurs or not as the value of [the](#)
 383 upwelling index (*UI*) exceeding 40 °C (in absolute values while *UI* is by definition a negative
 384 number). The upwelling events found using the selected criterion were also the occasions when
 385 the maximum negative temperature deviation from the transect mean value was at least -2 °C
 386 (except one event on 10-17 September 2007 when the maximum deviation was -1.97 °C).
 387 Furthermore, no other cases with negative temperature deviations exceeding -2 °C were detected.

388 Thus, the criterion $UI < -40$ °C gives quite similar results as would yield if using the criterion
389 based on the maximum negative temperature deviation of -2 °C.

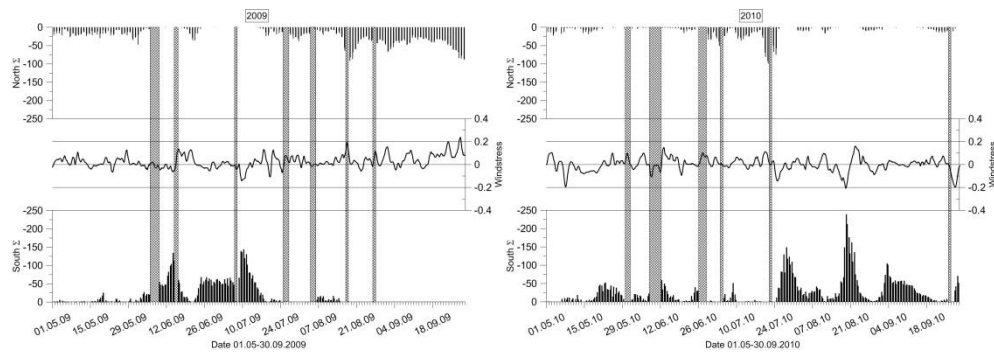
390
391 We identified in May-September 2007-2013 altogether 33 upwelling events, approximately half
392 of them (17) near the northern coast and half (16) near the southern coast (Table 2). The events
393 lasted from 3 days to 3 weeks, and the longest event was observed on 11-31 August 2013. On
394 average five events yearly were registered, and the maximum number of events (eight) was
395 observed in 2011. Based on available data, the number of days with the upwelling near the
396 northern coast was 150 and near the southern coast 140. As the total number of days with
397 measurements was 838, the upwelling occurred on 18 % and 17 % of days off the northern and
398 southern coast, respectively. The maximum negative temperature deviation from the mean value
399 was detected in August 2010 near the southern coast when it reached -7.78 °C. The largest
400 temperature deviation in the case of upwelling events near the northern coast of -6.15 °C was
401 detected in July 2013. The average of maximum temperature deviation was larger for the
402 upwelling events near the southern coast than near the northern coast— (-4.64 °C and -3.60 °C,
403 respectively).

404
405 While the maximum temperature deviation characterizes the peak of the upwelling, the
406 introduced cumulative upwelling index also takes into account the extent of the upwelling in
407 space and time. Regarding *CUI* the largest upwelling events were observed in 2013 – on 15-30
408 September 2013 off the southern coast ($CUI = -40.2$ °C day) and on 11-31 August 2013 off the
409 northern coast ($CUI = -39.7$ °C day). The upwelling events with the largest temperature deviation
410 in July-August 2010 were relatively short events lasting 7 days and gave respective *CUI* value as
411 -15.7 °C day and -20.8 °C day. The average *CUI* value of all upwelling events off the northern
412 coast was -14.5 °C day and off the southern coast -16.2 °C day. The sum of *CUI* values of all
413 detected upwelling events off the northern coast was -247.0 °C day and off the southern coast -
414 258.4 °C day.

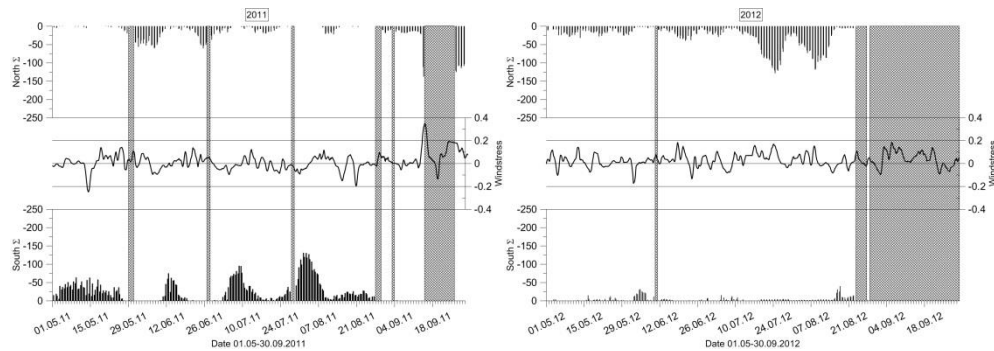
415



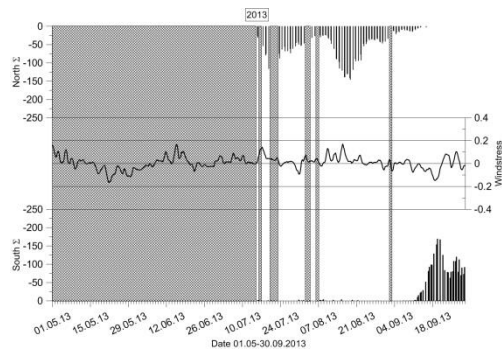
416



417



418



419

420

421

422

423

Figure 5. Temporal changes in upwelling index off the northern coast (upper columns at the top of each subplot; °C) and off the southern coast (lower columns at the bottom of each subplot; °C) and along-gulf wind stress (black curve in the middle; $N m^{-2}$) in May-September 2007 (a), 2008 (b), 2009 (c), 2010 (d), 2011 (e), 2012 (f) and 2013 (g).

424

425 The total *CUI* for all measurement days in 2007-2013 was -405.3 °C day for the northern coastal
426 area and -356.6 °C day for the southern coastal area. Thus, the negative temperature deviations
427 from the transect mean were more common for the northern coastal sea area while the upwelling
428 events were more intense in the southern coastal sea area. This feature is also well seen in Fig. 5
429 where e.g. in 2007 relatively low values of UI_N were found in most of the days near the northern
430 coast but only three upwelling events were revealed according to the criterion set in the present
431 study.

432
433 Seasonal variation of the frequency of occurrence and intensity of upwelling events ~~was~~
434 ~~revealed~~based on the analyzed data is as it follows. The highest number of events was observed
435 in July – 10 events, 5 off the northern coast and 5 off the southern coast, and the lowest in May –
436 4 events. The sum of *CUI* values of all events in July and August were -185.3 °C day and -
437 187.9 °C day, respectively, while it was only -28.6 °C day in May. In June and September, the
438 *CUI* of all events had intermediate magnitude —107.5 °C day and -137.0 °C day, respectively.
439 Obviously, the revealed seasonal course-trend was partly related to the temperature difference
440 between the surface layer and the cold layer beneath the seasonal thermocline, which has its
441 maximum in the Gulf of Finland in July-August (Liblik and Lips, 2011).

442

443 3.3 Upwelling characteristics in relation to wind forcing

444

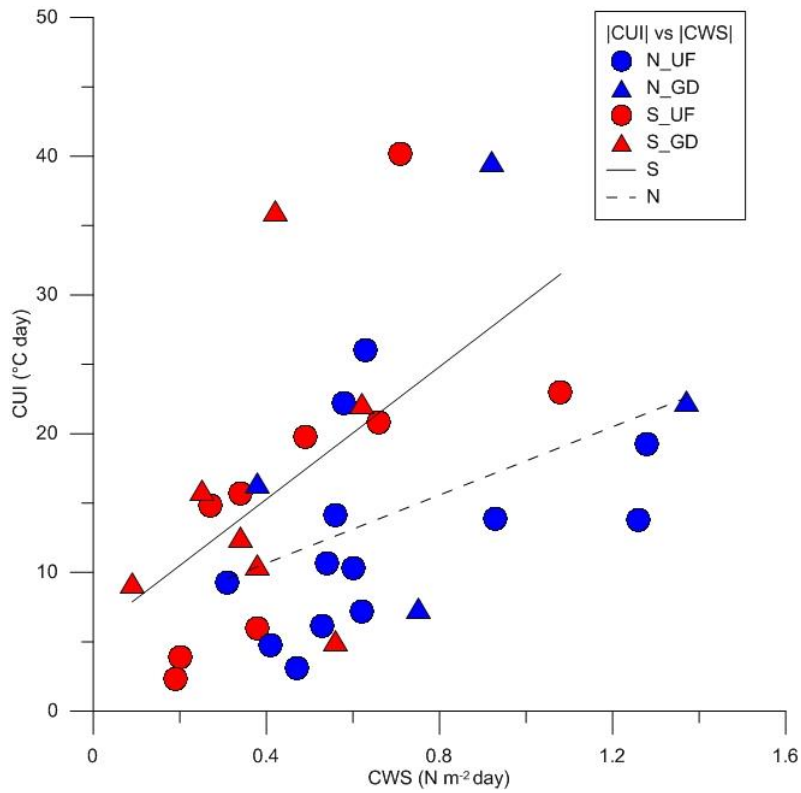
445 The occurrence of coastal upwelling events in the Gulf of Finland can be related quite well to the
446 variations of the along-gulf wind stress (Fig. 5). The upwelling events appeared after a certain
447 favorable wind pulses with long enough duration and magnitude. In the case of upwelling events
448 off the northern coast, the positive along-gulf wind stress was usually observed a few days before
449 the event and in the case of upwelling events off the southern coast, the wind stress was negative
450 for a few days (Fig. 5).

451

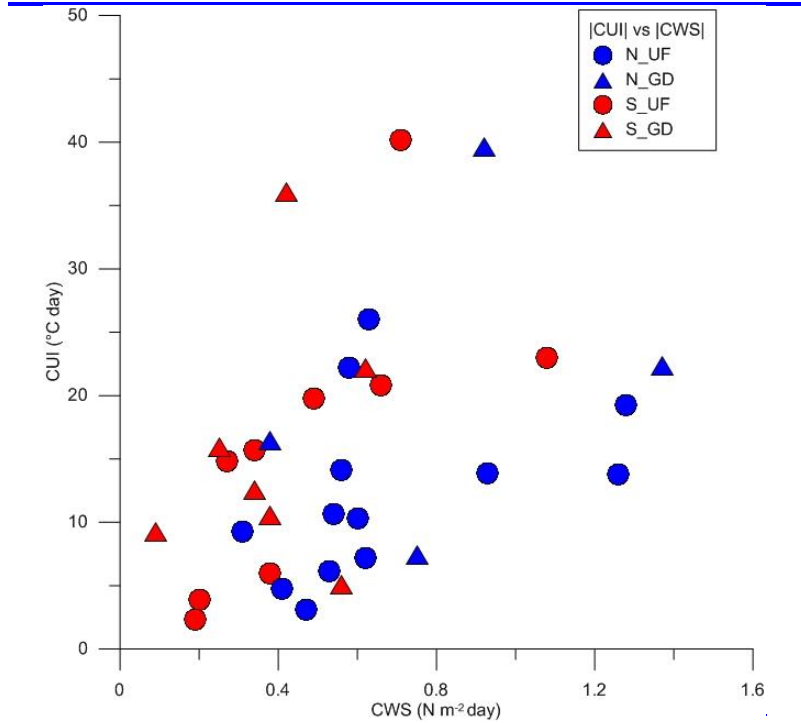
452 The estimated cumulative wind stress for the detected upwelling events varied between 0.31 and
453 1.37 N m⁻² day for westerly winds and between -0.09 and -1.08 N m⁻² day for easterly winds
454 (Table 2). The cumulative wind stress associated with each upwelling event was calculated based
455 on daily average wind stress values by summing them up from the first day with favorable wind

456 stress (within a period of 1 week before the event) to the last day with favorable wind stress
457 before the end of the event. If only one day with opposite wind stress appeared in a sequence in
458 the favorable wind stress series, then the calculation period was not broken. The average value of
459 the cumulative wind stress for an upwelling event off the northern coast was $0.71 \text{ N m}^{-2} \text{ day}$ and
460 off the southern coast $-0.44 \text{ N m}^{-2} \text{ day}$. It suggests that to produce a coastal upwelling event of an
461 equal magnitude the required favorable along-gulf wind stress has to be larger for the upwelling
462 events off the northern coast than for the events off the southern coast. This conclusion is drawn
463 by taking into account the above result that the average upwelling intensity (estimated as *CUI*)
464 was similar for the both coastal areas with slightly higher values of *CUI* for the upwelling events
465 off the southern coast. This suggestion is also supported by comparison of relationships between
466 the *CUI* and cumulative wind stress (*CWS*) related to the upwelling events near the opposite
467 coasts (Fig. 6). The linear regression lines between the *CUI* and *CSW* indicate that at the same
468 *CSW* values, Although the results are quite scattered, the upwelling events had higher intensities
469 off the southern coast occurred in conditions of lower *CWS* than off the northern coast.
470 Nevertheless, values and the maximum *CUI* near the southern coast was also found at lower
471 *CSW* than near the northern coast. the results are quite scattered, and the coefficient of
472 determination (r^2) between the *CUI* and *CSW* are 0.30 for the southern and 0.19 for the northern
473 upwelling events.

474



475



476

477

478

479

480

481

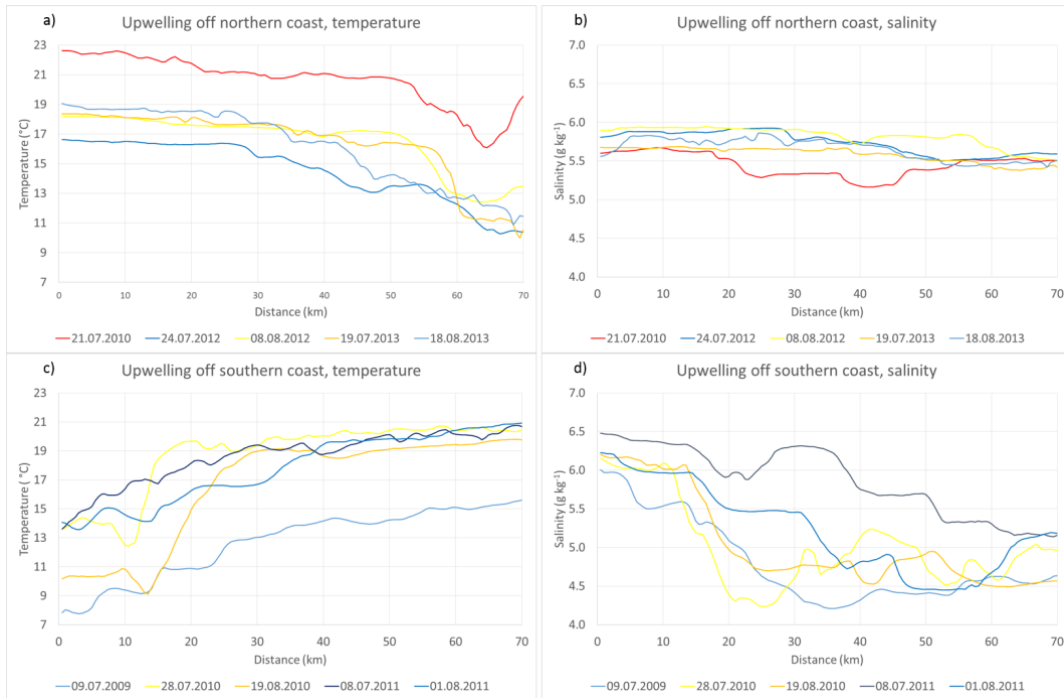
482

Figure 6. The relationship between the cumulative upwelling index (CUI) and cumulative along-gulf wind stress (CWS) based on 33 detected upwelling events in May-September 2007-2013. Red symbols indicate the events off the southern coast and blue symbols the events off the northern coast; circles correspond to the events with pronounced upwelling front (N_UP and C_UP) and triangles the events with a gradual decrease in temperature towards the coast (N_GD and S_GD). [The linear regression lines for southern \(solid line\) and northern upwelling events \(dashed line\) are shown.](#)

483 The average along-gulf wind stress for the entire study period from May to September in 2007-
484 2013 was 0.016 N m^{-2} . The seasonal averages had positive values in all studied years indicating
485 that the westerly-south-westerly winds prevailed in the region. The average values of wind stress
486 varied between 0.001 N m^{-2} in 2010 and 0.029 N m^{-2} in 2007, 2009 and 2012. In May-September
487 2010, when five upwelling events occurred off the southern coast and only one event off the
488 northern coast, the average along-gulf wind stress was close to zero indicating that the
489 cumulative wind forcing was almost equal from both directions. Furthermore, the wind stress
490 averaged over ~~the~~ all observed upwelling events in 2007-2013 was 0.015 N m^{-2} , which is very
491 close to the average wind stress over the entire study period. This estimate was obtained based
492 on the mean length of upwelling events of 8.8 days and mean cumulative wind stress values of
493 0.71 and $-0.44 \text{ N m}^{-2} \text{ day}$ off the northern and southern coasts, respectively. It can be concluded
494 that the difference between the wind impulses needed for the generation of upwelling events with
495 similar intensity near the opposite coasts is comparable to the average wind stress value in the
496 region.

497
498 Usually, the upwelling events occurred one or a few days after the start of the favorable wind
499 pulse, and the maximum of upwelling intensity was reached one or a few days after the
500 maximum wind stress (Fig. 5). ~~Daily measurements are too scarce to describe the temporal~~
501 ~~evolution of upwelling events in detail since the time required to initiate Ekman transport is~~
502 ~~shorter than or close to the inertial period (e.g. Lehmann and Myrberg, 2008) that is~~
503 ~~approximately 14 hours in the Gulf of Finland. Instead, w~~We made an attempt to reveal
504 characteristic spatial temperature and salinity distributions in the surface layer from coast to
505 coast at times of the maximum intensity of upwelling events. Surprisingly, the results did not
506 differ significantly between the northern and southern coast – two characteristic shapes of
507 upwelling events in the temperature distribution were identified for both coastal areas.

508



509

510

511

512

Figure 7. Characteristic distributions of temperature and salinity along the ferry route Tallinn-Helsinki with coastal upwelling events off the northern coast (a, b) and off the southern coast (c, d); x-axis shows the distance from the Tallinn Bay (latitude 59.48 N) in km along the meridional transect.

513

514

515

516

517

518

519

520

521

522

523

524

525

526

527

528

Mostly the upwelling events were characterized by a sharp and very intense temperature front between the upwelling waters and the rest of the transect (see Fig. 7 the yellow and orange curves). Typical for such events were an almost uniform temperature outside the upwelling area and the temperature minimum (maximum temperature deviation) close to the upwelling front. The other distribution pattern (blue curves in Fig. 7) exposed a gradual decrease of temperature towards the upwelling waters. Typical for the latter events were the irregularities in temperature distribution with a characteristic scale of a few kilometers and the temperature minimum (maximum temperature deviation) in the cell closest to the shore. In some cases, e.g. the event near the northern coast with maximum intensity on 18 August 2013 (see the light blue curve in Fig. 7 upper left panel), the observed temperature deviations were as large as during the upwelling events with strong temperature front. There was also a third type of temperature distribution when the upwelling waters were not attached to the shore (see red curve in Fig. 7 upper left panel) at least according to the measurements along the ferry route. All these types of upwelling events are well recognized on the maps of temporal changes of temperature and temperature deviation along the ferry route Tallinn-Helsinki (Figs. 2 and 4).

529

530 The spatial distribution of salinity in the surface layer from coast to coast drastically differed
531 between the upwelling events near the northern coast and the events near the southern coast (Fig.
532 7 right panels). In the latter case, both the salinity difference across the gulf and the spatial
533 variability at scales of a few to ten kilometers were much larger than in the former case. It is also
534 interesting that in the case of southern upwelling events, the salinity minimum along the transect
535 can be situated either very close to the upwelling front (e.g. on 28 July 2010) or near the northern
536 coast (e.g. 8 July 2011). Although such diverse patterns are partly related to the history of water
537 movements in the gulf, the salinity minimum (at least local minimum) close to the upwelling
538 front obviously is caused by the westward current jet along the front as also revealed by model
539 experiments (Laanemets et al., 2011). The salinity distribution across the gulf associated with the
540 northern upwelling events is very uniform with some variability at scales of a few to ten
541 kilometers, which have the amplitude several times less than spatial salinity variations associated
542 with the southern upwelling events.

543

544 | **4. DISCUSSION ~~AND CONCLUSIONS~~**

545

546 Several studies have shown how the Ferrybox measurements are successfully used for different
547 applications, such as for monitoring of coastal waters in combination with remote sensing
548 (Petersen et al., 2008), estimating carbon fluxes and primary productivity (Schneider et al., 2014)
549 and detecting cyanobacterial blooms (Seppälä et al., 2007). However, not enough attention is
550 paid to the Ferrybox systems, especially to the question how the results are affected by the used
551 technical solutions (like water intake depth and construction, piping, etc.). Furthermore, the
552 particularities of geographical location as well as the ferry route and schedule often determine
553 the most suitable applications and requirements for the data treatment. A good example of taking
554 advantage of the geographical location and ferry route is demonstrated by Buijsman and
555 Ridderinkhof (2007) who estimated the water and suspended matter exchange between the
556 Wadden Sea and the North Sea using data collected along the ferry route Den Helder – Texel.

557

558 The ferry route between Tallinn and Helsinki across the elongated Gulf of Finland and the
559 schedule consisting of two cruises a day and a short 1.5-hour stay in Helsinki made it possible to

560 introduce a procedure for correction of coordinates of measurement points and an additional
561 quality check routine for the collected data. The correlation between the data from the two
562 crossings on the same day should be high enough; otherwise, the data can be marked as
563 suspicious. We found that the highest correlation between the two datasets is achieved when the
564 data points are shifted by 3-4 minutes depending on the intake installation and the ferry. ~~We~~
565 ~~suggest that such coordinate correction procedure should be used in all Ferrybox systems.~~ This
566 analysis also demonstrates the confidence of the applied Ferrybox system even though the water
567 is taken in through a relatively large sea chest. Furthermore, the ferry route across the relatively
568 narrow gulf from coast to coast is very convenient to collect data on the offshore extension and
569 intensity of coastal upwelling events.

570
571 Various methods have been applied to reveal characteristic features of coastal upwelling events
572 in the Baltic Sea based on data mainly from remote sensing and numerical models. Data of high-
573 resolution long-term Ferrybox measurements have not been analyzed with this aim until now.
574 Certain temperature isoline as the border of the upwelling area was used by Uiboupin and
575 Laanemets (2009) and a temperature deviation (2 °C) from the mean temperature along zonal
576 transects was employed by Lehmann et al. (2012). The latter method is similar to the approach
577 applied in the present study, but we argue that the analysis of temperature deviations along
578 meridional transects is more appropriate in the Gulf of Finland. This conclusion is justified by
579 the fact that, on average, the north-south temperature gradient is negligible in the gulf (see Fig.
580 3a) while the west-east temperature gradient could exist between the shallower and narrower
581 Gulf of Finland and the deeper and wider Northern Baltic Proper due to differential warming and
582 cooling.

583
584 Nevertheless, it is interesting that our results on upwelling frequencies of about 17-18 % near the
585 northern and southern coast are very close to the results of Lehmann et al. (2012) if their results
586 based on remote sensing data were considered. They concluded that upwelling events were
587 present more than 15 % of time near the northern coast and about 15 % of time near the southern
588 coast. At the same time, the estimates of corresponding upwelling frequencies based on
589 numerical experiments differ from ~~those~~ values [obtained from the remote sensing data](#) and the
590 results of the present study. Based on model results, the northern coastal area has been suggested

591 as the main upwelling area in the Gulf of Finland with the upwelling occurrence up to 30 % of
592 time (Lehmann et al., 2012; Myrberg and Andrejev, 2003) while near the southern coast
593 downwelling should prevail (e.g. Myrberg and Andrejev, 2003). It shows that the models with
594 their current resolution and parameterization of sub-grid processes should be improved.

595
596 Analysis of wind data has also suggested that the coastal upwelling events should occur more
597 often off the northern coast of the Gulf of Finland than off the southern coast (Lehmann et al.,
598 2012; Uiboupin and Laanemets, 2009). The data set consisting of 838 days of measurements
599 from coast to coast used in the present analysis has revealed that, on average, the frequency of
600 upwelling events and their intensity are similar near the northern and southern coast of the gulf
601 although the wind data from the same period suggest prevalence of upwelling events off the
602 northern coast. Partly, this outcome can be explained by the higher position of the thermocline,
603 steeper bottom slope and greater depths in the southern part of the gulf as suggested by some
604 earlier studies (e.g. Väli et al., 2011; Laanemets et al. 2009). [Based on a simple theory of
605 upwelling dynamics linking the position of the onshore return flow with the bottom slope and
606 stratification \(Lentz and Chapman, 2004\), Laanemets et al. \(2009\) estimated that the return flow
607 should occur in the near-bottom layer for both northern and southern upwelling events in the
608 Gulf of Finland. Due to the steeper slope and greater depths, the upwelling outcome in the
609 vertical transport of cold and nutrient rich waters could be more intense in the southern gulf \(Väli
610 et al., 2011; Laanemets et al., 2009\).](#)

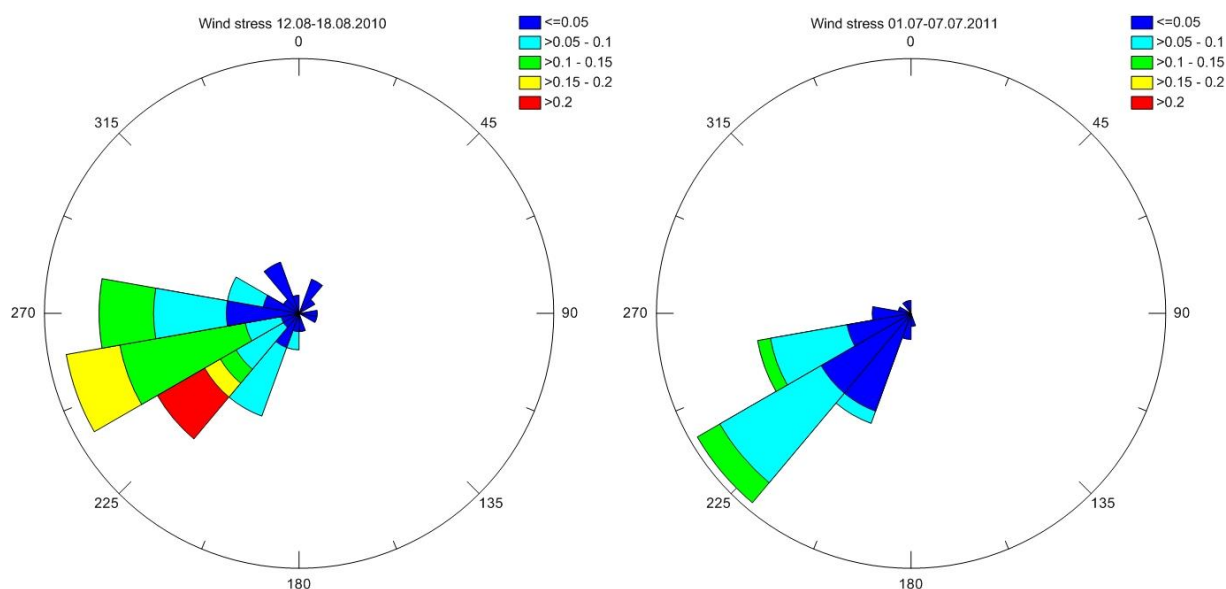
611
612 ~~However, one~~ [An alternative explanation](#) could be suggested if taking into account the estuarine
613 [character of the Gulf of Finland – the basin has free water exchange with the Baltic Proper in the](#)
614 [west while it is closed in the east where the main freshwater source is located. First, this basin](#)
615 [configuration and the prevalence of southwesterly winds together with the Coriolis force cause a](#)
616 [general cyclonic circulation in the surface layer of the gulf \(Alenius et al., 1998\). Such](#)
617 [circulation, in accordance with the geostrophic balance, yields in a higher sea level and deeper](#)
618 [thermocline at the northern part of the gulf \(e.g. see Andrejev et al., 2004\). A similar suggestion](#)
619 [was made by Liblik and Lips \(2016\) when they analyzed the relationship between the cross-gulf](#)
620 [inclination of the thermocline and wind forcing based on data from 35 cross-gulf CTD surveys](#)
621 [conducted in 2006-2013. that the thermohaline structure of the Gulf of Finland is adapted to the](#)

622 ~~general prevalence of westerly south westerly winds.~~ Thus, the wind impulse needed for the
623 ~~generation initiation~~ of a coastal upwelling event ~~of similar intensity~~ near the southern coast can
624 have a smaller magnitude. This suggestion is supported by the comparison of ~~average upwelling~~
625 ~~intensities expressed as the lowest cumulative upwelling index values and~~ cumulative wind stress
626 values, which have initiated ~~for the all~~ upwelling events ~~recorded~~ in 2007-2013 near the
627 ~~opposite two~~ coasts. The lowest CWS value related to an upwelling event along the northern coast
628 is larger than the CWS values for five upwelling events along the southern coast of the gulf(see
629 Fig. 6). A similar suggestion was made by Liblik and Lips (2016) on the basis of data analysis
630 from 35 cross-gulf CTD surveys conducted in 2006-2013.

631
632 Secondly, we suggest that for a stronger wind impulse during a longer period, the estuarine
633 character of the basin has a significant influence on the outcome. If the strong southwesterly
634 winds prevail, a downward movement of the thermocline in the gulf as a whole occurs since the
635 southwesterly winds cause inflow in the surface layer and outflow in the sub-surface layers (see
636 e.g. Elken et al., 2003; Lips et al., 2008b). In contrary, the down-estuary winds cause a general
637 upward movement of the thermocline in the gulf. Consequently, the up-estuary southwesterly
638 winds, on the one hand, cause upwelling along the northern coast, but on the other hand
639 downwelling in the gulf as a whole that could weaken the outcome. In the case of the down-
640 estuary easterly-northeasterly winds, a general upward movement of the thermocline in the gulf
641 supports the coastal upwelling along the southern coast. Such response of the water movements
642 to the forcing could be an explanation why, in general, the cumulative upwelling indexes
643 (presented in Fig. 6) increase faster with the strengthening of the favorable wind stress (CWS in
644 Fig. 6) for the southern upwelling events than for the northern upwelling events.

645
646 The average cross-gulf distributions of temperature and salinity were described based on the 7-
647 year data set of horizontal profiles. On average, the surface layer temperature did not have any
648 horizontal gradient while the surface layer salinity was higher in the southern part than in the
649 northern part of the gulf. The result that the surface water with the lowest salinity was on average
650 at about 20 km from the northern coast supports the suggested general circulation scheme in the
651 Gulf of Finland (e.g. Andrejev et al., 2004). At the same time, if the wind forcing favorable for
652 upwelling events near the southern coast prevailed (as it was observed in summer 2010) the low

653 salinity water appeared in the southern part of the open gulf, close to the upwelling front. This
 654 phenomenon was also observed during an intense upwelling event in August 2006 (Lips et al.,
 655 2009); it was modelled by Laanemets et al. (2011) and noted by Liblik and Lips (2016) based on
 656 an analysis of CTD data from surveys across the gulf in 2006-2013.
 657



658
 659 **Figure 8. Polar histogram of wind stress vectors ($N m^{-2}$) based on the wind data from a weekly period before the peak of upwelling events off**
 660 **the Estonian coast on [19-23 August 2010](#) (left panel) and [8-5-11 July 2011](#) (right panel).**

661
 662 The most intense upwelling events regarding temperature deviations were observed near the
 663 southern coast as it was also found by Uiboupin and Laanemets (2009, 2015). However, we did
 664 not identify clear differences in the temperature distribution patterns between the upwelling
 665 events off the two coasts. Instead, near the both coasts, the classical distribution with a sharp
 666 temperature front as well as the distribution characterized by a gradual decrease in temperature
 667 towards the coast have been observed. We [suggest that the latter type of temperature distribution](#)
 668 [could be associated with the development of upwelling filaments, which occurred and stayed in](#)
 669 [our measurement window for the several observed upwelling events.](#) ~~analyzed the wind data to~~
 670 ~~find out whether the forcing would be the reason for such different outcomes. Since often the~~
 671 ~~wind conditions were quite variable before the upwelling events, it was not possible to suggest~~
 672 ~~any quantitative criterion for wind forcing generating one or the other type of temperature~~
 673 ~~distribution.~~

674

675 In the case of the upwelling events along the southern coast, the wind speed was usually on
676 average higher before the events with the sharp temperature front (see Fig. 6 and Table 2). For
677 instance, the polar histograms of wind stress vectors shown in Fig. 8 are very similar except the
678 distribution of wind stress magnitudes. The period before the culmination of the upwelling event
679 with the sharp temperature front observed on 19 August 2010 had a large share of wind stress
680 values $> 0.15 \text{ N m}^{-2}$. ~~It allows us to suggest that the observed variability in spatial temperature~~
681 ~~distribution at the scales of a few kilometers could be related to sub-mesoscale motions, which~~
682 ~~are made visible if due to the slightly lower forcing the mesoscale dynamics do not fully~~
683 ~~dominate.~~ Nevertheless, the two prominent upwelling events along the northern coast – the most
684 intense event (on 11-31 August 2013) and the event corresponding to the largest cumulative
685 wind stress (on 18-27 July 2012), ~~and the most intense event along the northern coast~~ were both
686 characterized by the gradual decrease in temperature towards the coast (Fig. 6).

687

688 The filaments of upwelled waters are characteristic features of the upwelling events in the Gulf
689 of Finland (Uiboupin and Laanemets, 2009). Zhurbas et al. (2008) have shown based on a
690 numerical experiment that the cold/warm water squirts and filaments could develop after the
691 weakening of the upwelling favorable winds. Similarly, the squirts and filaments could develop
692 if the wind forcing is strong enough to initiate an upwelling event but not as strong as needed to
693 retain the mesoscale frontal dynamics. In the case of the southern upwelling events, it explains
694 why upwelling events with the gradual decrease of temperature mostly occurred when the wind
695 forcing was on average weaker.

696

697 As shown by Zhurbas et al. (2006), the baroclinic instability of the upwelling jet is expected to
698 occur when the bottom slope is smaller than the isopycnal slope. Thus, for the strongPartly, this
699 ~~result could be explained by~~ upwelling events, the filaments might appear with a higher
700 probability in the case of northern upwelling events since the bottom slope is about two times
701 shallower in the northern gulf than in the southern gulf (Uiboupin and Laanemets, 2009).
702 Furthermore, the probability of filament formation could be higher when the thermocline had a
703 deeper position that might enhance the influence of the bottom irregularities to the upwelling
704 dynamics. ~~the known estuarine dynamics of the Gulf of Finland where~~The prevailing strong

705 westerly-southwesterly winds, which cause an inflow in the upper layer and a compensating
706 outflow in the deeper layers (Elken et al., 2003; Liblik and Lips, 2012), could. ~~Thus, the winds~~
707 ~~favorable for upwelling events near the northern coast also~~ lead to the deepening of the seasonal
708 thermocline in the gulf in 2012 and 2013. The two very intense upwelling events with the
709 gradual temperature decrease were observed in these summers along the northern coast., ~~which~~
710 ~~works against the upwelling of sub-thermocline waters. Since the upwelling dynamics is~~
711 dependent on the vertical structure of the water column before the event (e.g. Lentz and
712 Chapman, 2004). ~~These suggestions have to be studied further in the future by combining~~
713 Ferrybox data (restricted to the surface layer and single transect) with the remote sensing and
714 water column data ~~since our measurements were restricted to the surface layer and single~~
715 ~~transect. It is known that the upwelling dynamics is very much dependent on the vertical~~
716 ~~structure of the water column before the event (e.g. Lentz and Chapman, 2004), and the~~
717 ~~filaments of upwelled waters are characteristic features of the upwelling events in the Gulf of~~
718 Finland (Uiboupin and Laanemets, 2009).

719

720 5. CONCLUSIONS

721

722 ~~In conclusion,~~ We showed that Ferrybox data from the Tallinn-Helsinki ferry route could be
723 successfully employed to describe the characteristics of coastal upwelling events in the Gulf of
724 Finland. An advantage of the geographical location of the ferry route across the relatively narrow
725 gulf and the schedule consisting of two crossings a day allowed to control the quality of the data
726 and introduce the upwelling index based on the data from a single crossing and the cumulative
727 upwelling index. In total, 33 coastal upwelling events were identified in May-September 2007-
728 2013. It is shown that the upwelling occurrences of 18 % and 17 % of days, as well as intensities
729 of upwelling events, are similar near the northern and southern coast. The most intense events
730 occur in July-August, most probably because of the warmest surface layer (strongest
731 thermocline) during those months. It is shown that the wind impulse needed to generate
732 upwelling events of similar intensity differs between the two coastal areas. We suggest that the
733 general thermohaline structure (adapted to the prevailing forcing) and the estuarine character of
734 the basin are reasons for the found different outcome. ~~that~~ The thermohaline structure of the
735 Gulf of Finland is characterized by a deeper position of the thermocline in the northern gulf;

736 thus, the upwelling initiation requires a stronger wind impulse there than in the southern coastal
737 area. Furthermore, the is-estuarine character of the basin leads to the weakening of the upwelling
738 created by the westerly (up-estuary) winds and strengthening of the upwelling created by the
739 easterly (down-estuary) winds. adapted to the prevailing forcing, and rather the deviation from
740 the average wind forcing than the absolute value of it should be considered when comparing the
741 wind impulses related to the upwelling generation. Two types of upwelling events were
742 identified – one characterized by a strong temperature (upwelling) front and the other revealing
743 gradual decrease of temperature from the open sea to the coastal area with maximum temperature
744 deviation very close to the shore. We suggest that the spatial variations in temperature with
745 scales of a few kilometers, which were characteristic for the latter type of upwelling events,
746 could be signs of sub-mesoscale motions the meso- and sub-mesoscale features (filaments and
747 squirts) associated with the upwelling dynamics.

748

749 **Acknowledgements**

750

751 We are grateful to Tallink (Estonia) for the possibility to conduct the measurements on board the
752 ferries. We thank our colleagues, especially Inga Lips and Fred Buschmann, for their help in
753 maintaining the Ferrybox system, and Taavi Liblik for his suggestions regarding data processing.
754 This work was supported by institutional research funding IUT19-6 of the Estonian Ministry of
755 Education and Research and by EU Regional Development Foundation, Environmental
756 Conservation and Environmental Technology R&D Programme project VeeOBS (3.2.0802.11-
757 0043).

758

759 **References**

760

- 761 Alenius, P., Myrberg, K., Nekrasov, A. 1998. The physical oceanography of the Gulf of Finland:
762 a review. *Boreal Environ. Res.*, 3, 97–125.
- 763 Andrejev, O., Myrberg, K., Alenius, P., Lundberg, P.A., 2004. Mean circulation and water
764 exchange in the Gulf of Finland - a study based on three-dimensional modeling. *Boreal*
765 *Environ. Res.*, 9(1), 1–16.

766 Buijsman, M.C., Ridderinkhof, H., 2007. Long-term ferry-ADCP observations of tidal currents
767 in the Marsdiep inlet. *J. Sea Res.*, 57, 237–256.

768 Elken, J., Raudsepp, U., Lips, U., 2003. On the estuarine transport reversal in deep layers of the
769 Gulf of Finland. *J. Sea Res.* 49, 267–274.

770 Haapala, J. 1994. Upwelling and its influence on nutrient concentration in the coastal area of the
771 Hanko Peninsula, entrance of the Gulf of Finland. *Est. Coast. Shelf Sci.*, 38(5), 507–521.

772 Hardman-Mountford, N. J., Moore, G., Bakker, D. C. E., Watson, A. J., Schuster, U., Barciela,
773 R., Hines, A., Moncoiffe', G., Brown, J., Dye, S., Blackford, J., Somerfield, P. J., Holt,
774 J., Hydes, D. J., and Aiken, J. 2008. An operational monitoring system to provide
775 indicators of CO₂- related variables in the ocean. – *ICES Journal of Marine Science*, 65,
776 1498–1503.

777 Keevallik, S., Soomere, T., 2010. Towards quantifying variations in wind parameters across the
778 Gulf of Finland. *Estonian Journal of Earth Sciences*, 59(4), 288–297.

779 Kononen, K., Kuparinen, J., Mäkela, K., Laanemets, J., Pavelson, J., Nõmmann, S., 1996.
780 Initiation of cyanobacterial blooms in a frontal region at the entrance to the Gulf of
781 Finland, Baltic Sea. *Limnol. Oceanogr.*, 41, 98–112.

782 Laanemets, J., Väli, G., Zhurbas, V., Elken, J., Lips, I., Lips, U., 2011. Simulation of mesoscale
783 structures and nutrient transport during summer upwelling events in the Gulf of Finland
784 in 2006 *Boreal Environ. Res.*, 16A, 15–26.

785 Laanemets, J., Zhurbas, V., Elken, J., Vahtera, E., 2009. Dependence of upwelling-mediated
786 nutrient transport on wind forcing, bottom topography and stratification in the Gulf of
787 Finland: model experiments. *Boreal Environ. Res.*, 14, 213–225.

788 Lehmann, A., Myrberg, K., Höflich, K., 2012. A statistical approach to coastal upwelling based
789 on the analysis of satellite data for 1990-2009. *Oceanologia*, 54, 369-393.

790 Lehmann, A., Myrberg, K., 2008. Upwelling in the Baltic Sea – A review. *J. Marine Syst.*, 74,
791 S3–S12.

792 Lentz, S.J., Chapman, D.C., 2004. The importance of nonlinear cross-shelf momentum flux
793 during wind-driven coastal upwelling. *J. Phys. Oceanogr.*, 34, 2444–2457.

794 Liblik, T., Lips, U., 2016. Variability of pycnoclines in a three-layer, large estuary: the Gulf of
795 Finland. *Boreal Environ. Res.* (in press).

796 Liblik, T., Lips, U., 2012. Variability of synoptic-scale quasi-stationary thermohaline
797 stratification patterns in the Gulf of Finland in summer 2009. *Ocean Sci.*, 8, 603–614.

798 Liblik, T., Lips, U., 2011. Characteristics and variability of the vertical thermohaline structure in
799 the Gulf of Finland in summer. *Boreal Environ. Res.*, 16A, 73–83.

800 Lips, I., Lips, U. 2008. Abiotic factors influencing cyanobacterial bloom development in the
801 Gulf of Finland (Baltic Sea). *Hydrobiologia*, 614, 133–140.

802 Lips, I., Lips, U., Liblik, T. 2009. Consequences of coastal upwelling events on physical and
803 chemical patterns in the central Gulf of Finland (Baltic Sea). *Cont. Shelf Res.* 29, 1836–
804 1847.

805 ~~Lips, U., Lips, I., Kikas, V., Kuvaldina, N., 2008. Ferrybox measurements: a tool to study meso-~~
806 ~~scale processes in the Gulf of Finland (Baltic Sea)~~

807 Lips, U., Lips, I., Kikas, V., Kuvaldina, N., 2008a. Ferrybox measurements: a tool to study
808 meso-scale processes in the Gulf of Finland (Baltic Sea). *US/EU-Baltic Symposium,*
809 *Tallinn, 27-29 May, 2008. IEEE, (IEEE Conference Proceedings), 1 - 6.*

810 ~~Lips, U., Lips, I., Kikas, V., Liblik, T., Kuvaldina, N., Elken, J., 2008b. Ferrybox measurements: a~~
811 ~~tool to study meso-scale processes~~ [Estuarine transport versus vertical movement and](#)
812 [mixing of water masses in the Gulf of Finland \(Baltic Sea\). US/EU-Baltic Symposium,](#)
813 [Tallinn, 27-29 May, 2008. IEEE, \(IEEE Conference Proceedings\), 1 - 8.](#)

814 Männik, A., Merilain, M., 2007. Verification of different precipitation forecasts during extended
815 winter-season in Estonia. *HIRLAM Newsletter*, No. 52, 65–70.

816 Myrberg, K., Lehmann, A., Raudsepp, U., Szymelfenig, M., Lips, I., Lips, U., Matciak, M.,
817 Kowalewski, M., Krezel, A., Burska, D., Szymanek, L., Ameryk, A., Bielecka, L.,
818 Bradtke, K., Galkowska, A., Gromisz, S., Jedrasik, J., Kaluzny, M., Kozłowski, L.,
819 Krajewska-Soltys, A., Oldakowski, B., Ostrowski, M., Zalewski, M., Andrejev, O.,
820 Suomi, I., Zhurbas, V., Kauppinen, O.-K., Soosaar, E., Laanemets, J., Uiboupin, R.,
821 Talpsepp, L., Golenko, M., Golenko, N., Vahtera, E., 2008. Upwelling events, coastal
822 offshore exchange, links to biogeochemical processes – Highlights from the Baltic Sea
823 Science Congress at Rostock University, Germany, 19-22 March 2007. *Oceanologia*, 50,
824 95-113.

825 Myrberg, K., Andrejev, O. 2003. Main upwelling regions in the Baltic Sea – a statistical analysis
826 based on three-dimensional modeling. *Boreal Environ. Res.*, 8(2), 97-112.

827 Paerl, H.W., Rossignol, K.L., Guajardo, R., Hall, N.S., Joyner, A., Peierls, B.L., Ramus, J.S.
828 2009. FerryMon: Ferry-Based Monitoring and Assessment of Human and Climatically
829 Driven Environmental Change in the Albemarle-Pamlico Sound System. *Environ. Sci.*
830 *Technol.*, 43, 7609–7613

831 Pavelson, J., Laanemets, J., Kononen, K., S. Nõmman, 1997. Quasi-permanent density front at
832 the entrance to the Gulf of Finland: Response to wind forcing. *Cont. Shelf Res.*, 17, 253-
833 265.

834 Petersen, W., 2014. FerryBox systems: State-of-the-art in Europe and future development. *J.*
835 *Marine Syst.*, 140, 4-12.

836 Petersen W., Wehde, H., Krasemann, H., Colijn, F., Schroeder, F., 2008. FerryBox and MERIS –
837 Assessment of coastal and shelf sea ecosystems by combining in situ and remotely sensed
838 data. *Est. Coast. Shelf Sci.*, 77, 296-307.

839 Rantajarvi, E. (Ed.) 2003. Alg@line in 2003: 10 years of innovative plankton monitoring and
840 research and operational information service in the Baltic Sea. *MERI – Report Series of*
841 *the Finnish Institute of Marine Research*, No. 48, 1-36.

842 Schneider, B., Gülzow, W., Sadkowiak, B., Rehder, G., 2014. Detecting sinks and sources of
843 CO₂ and CH₄ by ferrybox-based measurements in the Baltic Sea: Three case studies. *J.*
844 *Marine Syst.*, 140, 13-25.

845 Seppälä, J., Ylöstalo, P., Kaitala, S., Hällfors, S., Raateoja, P., Maunula, P., 2007. Ship-of-
846 opportunity based phycocyanin fluorescence monitoring of the filamentous cyanobacteria
847 bloom dynamics in the Baltic Sea. *Est. Coast. Shelf Sci.*, 73, 489-500.

848 Talpsepp, L., Nõges, T., Raid, T., Kõuts, T. 1994. Hydrophysical and hydrobiological processes
849 in the Gulf of Finland in summer 1987 – characterization and relationship. *Cont. Shelf*
850 *Res.*, 14, 749-763.

851 Uiboupin, R., Laanemets, J., 2009. Upwelling characteristics derived from satellite sea surface
852 temperature data in the Gulf of Finland, Baltic Sea, *Boreal Environ. Res.*, 14 (2), 297-
853 304.

854 Uiboupin, R., Laanemets, J., 2015. Upwelling parameters from bias-corrected composite satellite
855 SST maps in the Gulf of Finland (Baltic Sea). *IEEE Geoscience and Remote Sensing*
856 *Letters*, 12, 592-596.

857 Vahtera, E., Laanemets, J., Pavelson, J., Huttunen, M., Kononen, K., 2005. Effect of upwelling
 858 on the pelagic environment and bloom-forming cyanobacteria in the Western Gulf of
 859 Finland, Baltic Sea. *J. Marine Syst.*, 58, 67-82.

860 Väli, G., 2011. Numerical experiments on matter transport in the Baltic Sea. PhD thesis, Tallinn
 861 Technical University Press.

862 Väli, G., Zhurbas, V., Laanemets, J., Elken, J., 2011. Simulation of nutrient transport from
 863 different depths during an upwelling event in the Gulf of Finland. *Oceanologia*, 53, 431-
 864 448.

865 [Zhurbas, V., Laanemets, J., Vahtera, E., 2008. Modeling of the mesoscale structure of coupled
 866 upwelling/downwelling events and the related inputs of nutrients to the upper mixed layer
 867 in the Gulf of Finland, Baltic Sea. *J. Geophys. Res.*, 113, C05004, doi:
 868 \[10.1029/2007JC004280\]\(https://doi.org/10.1029/2007JC004280\).](#)

869 [Zhurbas, V.M., Oh, I.S., Park, T., 2006. Formation and decay of a longshore baroclinic jet
 870 associated with transient coastal upwelling and downwelling: a numerical study with
 871 application to the Baltic Sea. *J. Geophys. Res.*, 111, C04014, doi:
 872 \[10.1029/2005JC003079\]\(https://doi.org/10.1029/2005JC003079\).](#)

873
874
875
876
877

878 **Table 1.** Periods of measurements along the ferry route Tallinn-Helsinki in 2007-2013, number
 879 of days with measurements and number of days with upwelling events off the northern coast (N)
 880 and off the southern coast (S).

Year	Ferry	Period	Number of days with data	Number of days with upwelling	
				N	S
2007	Galaxy	1 May – 30 September	141	26	21
2008	Galaxy	1 May – 13 July	90	8	11
	Baltic Princess	13 August – 30 September			
2009	Baltic Princess	1 May – 30 September	145	33	30
2010	Baltic Princess	1 May – 30 September	140	5	32

2011	Baltic Princess	1 May – 30 September	135	19	30
2012	Baltic Princess	1 May – 28 August	113	22	0
2013	Silja Europa	15 July – 30 September	74	37	16

881

882

883 **Table 2.** Characteristics of detected upwelling events; dates, coastal area (N – off northern coast;
884 S – off southern coast), type (UF – with strong upwelling front, GD - - with gradual decrease of
885 temperature), maximum temperature deviation from the transect mean value, cumulative
886 upwelling index calculated for each event and cumulative along-gulf wind stress calculated for
887 upwelling favourable winds before and during the upwelling event.

No	Dates	Coast	Type	Maximum temperature deviation (°C)	Cumulative upwelling intensity (°C day)	Cumulative wind stress (N m ⁻² day)
1.	3-14 June 2007	S	UF	-4.12	-19.8	-0.49
2.	8-16 July 2007	S	GD	-3.02	-12.6	-0.34
3.	21-27 July 2007	N	UF	-4.02	-13.9	0.93
4.	29 July – 8 August 2007	N	GD	-3.64	-16.5	0.38
5.	10-17 September 2007 ⁽¹⁾	N	GD	-1.97	-7.5	0.75
6.	26-28 May 2008 ⁽²⁾	S	UF	-2.52	-3.9	-0.20
7.	11-15 June 2008	N	UF	-2.73	-7.2	0.62
8.	27-29 June 2008	N	UF	-2.27	-6.2	0.53
9.	10-17 September 2008	S	UF	-5.42	-23.0	-1.08
10.	9-16 June 2009	S	UF	-4.77	-14.8	-0.27
11.	24 June – 14 July 2009	S	GD	-5.78	-36.1	-0.42
12.	16-22 August 2009	N	UF	-3.20	-10.7	0.54
13.	28 August – 9 September 2009	N	UF	-2.74	-14.1	0.56
14.	17-30 September 2009 ⁽³⁾	N	UF	-3.09	-19.3	1.28
15.	20-24 May 2010	S	GD	-2.21	-5.1	-0.56
16.	12-13 June 2010 ⁽⁴⁾	S	UF	-2.60	-2.3	-0.19
17.	20-24 July 2010	N	UF	-4.70	-9.3	0.31
18.	26 July – 1 August 2010	S	UF	-6.19	-15.7	-0.34
19.	17-23 August 2010	S	UF	-7.78	-20.8	-0.66
20.	2-12 September 2010	S	GD	-5.27	-16.0	-0.25
21.	4-12 May 2011 ⁽⁵⁾	S	GD	-2.22	-9.3	-0.09
22.	31 May – 8 June 2011	N	UF	-2.32	-10.3	0.60
23.	11-15 June 2011	S	UF	-3.12	-6.0	-0.38
24.	24-27 June 2011	N	UF	-2.40	-4.8	0.41
25.	5-10 July 2011	S	GD	-5.05	-10.6	-0.38
26.	29 July – 7 August 2011	S	GD	-4.69	-22.2	-0.62

27.	14 September 2011 ⁽⁶⁾	N	UF	-4.90	-3.1	0.47
28.	26-30 September 2011 ⁽⁷⁾	N	UF	-3.27	-13.8	1.26
29.	18-27 July 2012 ⁽⁸⁾	N	GD	-4.55	-22.4	1.37
30.	2-13 August 2012	N	UF	-4.17	-22.2	0.58
31.	17 July – 1 August 2013 ⁽⁹⁾	N	UF	-6.15	-26.0	0.63
32.	11-31 August 2013	N	GD	-5.03	-39.7	0.92
33.	15-30 September 2013	S	UF	-7.34	-40.2	-0.71

888

889 ⁽¹⁾ temperature deviation was less than -2 °C during the event on 10-17 September 2007

890 ⁽²⁾ data absent before 26 May 2008 for more than 1 day

891 ⁽³⁾ data analysed until 30 September 2009 (upwelling event did further)

892 ⁽⁴⁾ data absent before 12 June 2010 for more than 1 day

893 ⁽⁵⁾ early spring with possible contribution of difference in surface water warming

894 ⁽⁶⁾ no data available after 14 September 2011

895 ⁽⁷⁾ no data available before 26 September 2011, wind data missing on 24-26 September 2011

896 ⁽⁸⁾ wind data on 14-15 July 2012 not available

897 ⁽⁹⁾ ferrybox data on 20-21 July 2013 not available

898

899

900

901

902 **Figure captions**

903

904 **Figure 1.** Map of the Baltic Sea (a) and the study area with the Ferrybox transect and

905 Kalbadagrund meteorological station.

906

907 **Figure 2.** Temporal changes of temperature (in °C) and salinity (in g kg⁻¹) distributions between

908 Tallinn and Helsinki from 1 May to 30 September in 2007 (a, b), 2008 (c, d), 2009, (e, f), 2010

909 (g, h), 2011 (i, j), 2012 (k, l) and 2013 (m, n); y-axis shows the distance from the Tallinn Bay

910 (latitude 59.48 N) in km along the meridional transect.

911

912 **Figure 3.** Distributions of temperature (in °C) and salinity (in g kg⁻¹) deviations from the [daily](#)

913 transect mean value along the ferry route Tallinn-Helsinki for all measurements in May-

914 September 2007-2013 (a, b), 2009 (c, d) and 2010 (e, f). Mean values for each 0.5-km cell (solid

915 curves) and plus/minus RMSE (dashed curves) are shown; x-axis shows the distance from the
916 Tallinn Bay (latitude 59.48 N) in km along the meridional transect.

917
918 **Figure 4.** Temporal changes of spatial distributions of temperature deviations (in °C) from the
919 daily transect mean value between Tallinn and Helsinki from 1 May to 30 September in 2007 (a),
920 2008 (b), 2009, (c), 2010 e), 2011 (f), 2012 (g) and 2013 (h); y-axis shows the distance from the
921 Tallinn Bay (latitude 59.48 N) in km along the meridional transect.

922
923 **Figure 5.** Temporal changes of upwelling index off the northern coast ([at the top of each](#)
924 [subplotupper columns](#); °C) and off the southern coast ([at the bottom of each subplotlower](#)
925 [columns](#), °C) and along-gulf wind stress (black curve in the middle; N m^{-2}) in May-September
926 2007 (a), 2008 (b), 2009 (c), 2010 (d), 2011 (e), 2012 (f) and 2013 (g).

927
928 **Figure 6.** Relationship between the cumulative upwelling index (CUI) and cumulative along-
929 gulf wind stress (CWS) based on 33 detected upwelling events in May-September 2007-2013.
930 Red symbols indicate the events off the southern coast and blue symbols the events off the
931 northern coast; circles correspond to the events with pronounced upwelling front (N_UF and
932 C_UF) and triangles the events with gradual decrease of temperature towards the coast (N_GD
933 and S_GD). [The linear regression lines for southern \(solid line\) and northern upwelling events](#)
934 [\(dashed line\) are shown.](#)

935
936 **Figure 7.** Characteristic distributions of temperature and salinity along the ferry route Tallinn-
937 Helsinki with coastal upwelling events off the northern coast (a, b) and off the southern coast (c,
938 d); x-axis shows the distance from the Tallinn Bay (latitude 59.48 N) in km along the meridional
939 transect.

940
941 **Figure 8.** Polar histogram of wind stress vectors (N m^{-2}) based on the wind data from a weekly
942 period before the peak of upwelling events off the Estonian coast on [19-17-23 August 2010 \(left](#)
943 [panel\)](#) and [8-5-11 July 2011 \(right panel\)](#).

944